Heterogeneity of tyrosine hydroxylase expressing neurons in the main olfactory bulb of the mouse

Toshio Kosaka, Angela Pignatelli, Katsuko Kosaka

PII: S0168-0102(19)30471-7

DOI: https://doi.org/10.1016/j.neures.2019.10.004

Reference: NSR 4313

To appear in: *Neuroscience Research*

Received Date: 19 August 2019

Revised Date: 29 September 2019

Accepted Date: 4 October 2019

Please cite this article as: Kosaka T, Pignatelli A, Kosaka K, Heterogeneity of tyrosine hydroxylase expressing neurons in the main olfactory bulb of the mouse, *Neuroscience Research* (2019), doi: https://doi.org/10.1016/j.neures.2019.10.004

Heterogeneity of tyrosine hydroxylase expressing neurons in the main olfactory bulb of the mouse.

Running title: Heterogeneity of DA-GABAergic neurons in MOB

Toshio Kosaka[1], Angela Pignatelli[2], Katsuko Kosaka[3]

[1]Department of Medical Science Technology, Faculty of Health and Welfare Sciences in Fukuoka, International University of Health and Welfare, 137-1 Enokizu, Okawa City, Fukuoka 831-8501, Japan

[2] Department of Biomedical and Specialty Surgical Sciences, Physiology Section, University of Ferrara, Via Borsari 46, Ferrara, Italy

[3] Department of Physical Therapy, Fukuoka International University of Health and Welfare, 3-6-40 Momochihama, Sawara-ku, Fukuoka 814-0001, Japan

Corresponding author: Toshio Kosaka

Department of Medical Science Technology, Faculty of Health and Welfare Sciences in Fukuoka, International University of Health and Welfare, 137-1 Enokizu, Okawa City, Fukuoka 831-8501, E mail: t-kosaka@iuhw.ac.jp Tel. 0944-89-2000

Highlights

- DA-GABAergic neurons cluster in GL but also scattered in EPL~GCL.
- In GL there are 4 distinct types of DA-GABAergic neurons and other unclassified neurons.
- DA-GABAergic large PG cells are the main source of the interglomerular connections.
- There are both axonic and anaxonic DA-GABAergic small PG cells.
- Dendrites of some DA-GABAergic neurons in EPL~GCL participate to the GL neuropil.

Abstract

The structural features of dopamine (DA)-GABAergic neurons in the mouse main olfactory bulbs were examined, using both wild type and transgenic TH-GFP mice, with the combination of several methods; the immunocytochemistry, biotinylated dextran amine labeling, lucifer yellow injection in fixed slices, biocytin injection in live slice and the functional olfactory deprivation. DA-GABAergic neurons were clustered in the glomerular layer (GL) but they also scattered in other layers. DA-GABAergic juxtaglomerular neurons, were classified into 5 groups based on their structural features and named as follows: 1) Large periglomerular (LPG) cells with tuft-like glomerular dendritic branches and apparent axons extending to the distant glomeruli, which correspond to the " inhibitory juxtaglomerular association (IJGA) neurons" participating in the interglomerular association system. 2) Small periglomerular (SPG) cells including both axonic and anaxonic ones; the axonic SPG cells might correspond to the classical periglomerular cells. 3) Transglomerular cells extending dendritic

processes spanning 2 or more glomeruli. 4) Incrusting cells extending their dendritic branches mainly in the periphery of the glomeruli. 5) Other various neurons not-yet classified. In the layers other than the GL various types of TH expressing neurons were scattered; some of them extended dendritic processes into the GL.

Abbreviations

ABC, avidin-biotin-peroxidase complex

ACSF, artificial cerebrospinal fluid

AIS, axon initial segment

AnkG, ankyrin G

AOB, accessory olfactory bulb

BDA, biotinylated dextran amine

BSA, bovine serum albumin

CB, calbindin D28k

CLSM, confocal laser scanning microscope

CTB, cholera toxin B subunit

Cy3, indocarbocyanine

Cy5, indodicarbocyanine

DA, dopamine

DAB, diaminobenzidine tetrahydrochloride

DAPI, 4',6-diamidino-2-phenylindole

DIC, differential interference contrast

EGTA, ethylene glycol tetraacetic acid

EPL, external plexiform layer

FITC, fluorescein isothiocyanate

GAD, glutamic acid decarboxylase

GCL, granule cell layer

GFP, green fluorescent protein

GL, glomerular layer

IPL, internal plexiform layer

JG, juxtaglomerular

LPG, large periglomerular

LY, lucifer yellow

MCL, mitral cell layer

MOB, main olfactory bulb

NA, numerical aperture

NOS, nitric oxide synthase

OB, olfactory bulb

OMP, olfactory marker protein

ON, olfactory nerve & olfactory nerve terminal

ONL, olfactory nerve layer

PB, phosphate buffer

PBS, phosphate buffered saline

PG, periglomerular

PV, parvalbumin

SCGN, secretagogin

SPG, small periglomerular

TG, transglomerular

TH, tyrosine hydroxylase

VGluT, vesicular glutamate transporter

Keywords: glomerulus; immunohistochemistry; Ankyrin G; axon; axon initial segment; dendrite; short-axon cell.

1. Introduction

Among the neurons in the main olfactory bulbs (MOBs) of the rodents dopaminergic neurons might be most controversial. As we summarized previously (Kosaka and Kosaka, 2011, 2016), once the dopaminergic juxtaglomerular (JG) neurons

had been classified into two groups, the larger one as the external tufted cells, presumed excitatory neurons, and the smaller one as the periglomerular (PG) cells, inhibitory neurons (Halász et al. 1981; Davis and Macrides 1983). However, it turned out that almost of both larger and smaller types of dopaminergic JG neurons were GABAergic (Kosaka et al. 1985, 1987, Gall et al. 1987), that is, they were "DA-GABAergic JG neurons." The GABAergic nature of dopaminergic JG neurons in the OBs was further confirmed in transgenic mice (Parrish-Aungst et al., 2007; Panzanelli et al. 2007; Maher and Westbrook, 2008). Furthermore the co-transmission of GABA and DA in dopaminergic JG neurons of the transgenic mouse MOBs was confirmed physiologically (Maher and Westbrook, 2008). Recent functional analyses revealed the importance of DA-GABAergic JG neurons in the control of glomerular outputs in the MOBs (Banerjee et al., 2015; Liu et al., 2016; Vaaga et al., 2017; Shao et al., 2019: for review, Pignatelli and Belluzzi, 2017; Burton, 2017). On the other hand there appears to be a disagreement about the neuron types of these DA-GABAergic JG neurons among research groups. It seems that this disagreement might be caused from the ambiguity in the structural features of DA-GABAergic JG neurons, especially in the differentiation of the dendrites and axons. For example some groups named the DA-GABAergic JG neurons as "short-axon cells" without identifying axons or confirming the presence of axons (Kiyokage et al. 2010; Bywalez et al. 2017). Previously we

classified the DA-GABAergic JG neurons into two groups, the larger and smaller ones, and showed that the larger type of DA-GABAergic JG neurons extended their axonal processes to distant glomeruli and thus were the major source of the interglomerular association (Kosaka and Kosaka, 2008b, 2011, 2016) and further that the larger and smaller types of DA-GABAergic JG neurons were different in their time of origin (Kosaka and Kosaka, 2009). These previous observations were also confirmed by other research groups (Kiyokage et al. 2010; Galliano et al. 2018).

In the present study we examined the structural features of DA-GABAergic JG neurons and those in other layers in the mouse MOBs. We especially intended to reveal the structural details of heterogeneous DA-GABAergic JG neurons.

2. Materials and methods

2-1. General tissue preparations

All experiments performed in Japan were carried out in accordance with “the Fundamental Guidelines for Proper Conduct of Animal Experiment and Related Activities in Academic Research Institutions” of the Ministry of Education, Culture, Sports, Science and Technology of Japan, the "Guide for the Care and Use of Laboratory Animals 8th edition (2011)" and the institutional guidance for animal welfare (the Guidelines for Animal Experiment in International University of Health

and Welfare). Every experimental procedure was approved by the Committee of the Ethics on Animal Experiment in International University of Health and Welfare.

The biocytin injection experiments on the live slices from TH-GFP mice were carried out in Ferrara University, Italy. Experimental procedures were designed so as to reduce the number of animals used and their sufferance. Care and use of animals was conducted according to guidelines established by European Council (63/2010) and Italian laws (D.Lgsl 26/2014) on the protection of animals used for scientific purposes. The experimental protocols were ratified by the Committee for Animal Welfare of the University of Ferrara (OBA), by the Directorate - General for Animal Health of the Italian Ministry of Health, and were supervised by the Campus Veterinarian of the University of Ferrara.

In this study we used wild type C57BL/6J mice (Japan SLC, Inc.) and TH-GFP mice (B6.B6D2-Tg (Th-EGFP)21-31Koba RBRC02095, Riken; Sawamoto et al., 2001; Matsushita et al., 2002). For the fixation the animals were deeply anesthetized with sodium pentobarbital (100 mg/kg) and perfused transcardially with phosphate buffered saline (PBS, pH 7.4) followed by 4% paraformaldehyde in 0.1 M phosphate buffer (PB, pH 7.4). The brains were left in situ for 1-2 hours at room temperature, then removed from the skull and stocked for overnight in the same fixative at 7°C. The brains were dissected out, encapsulated in 4 % agar in PBS and cut into 50 or 150 µm-thick serial

sections on a vibratome (Leica VT1000S). Then 50 µm-thick sections were processed for either ABC-DAB method or the multiple-fluorescent immunolabeling and 150 µm-thick were for lucifer yellow injections as described later.

For the ABC-DAB method sections were incubated in 3% H_2O_2 in 80% methanol for 1~2hours, rinsed with PBS, then incubated in the blocking/dilution solution consisting of 10% horse serum, 1% bovine serum albumin (BSA), 0.3% Triton X and 0.05% sodium azide in PBS overnight. Then they were incubated in rabbit anti-TH (1: 100,000, gift from Dr. Nagatsu; Nagatsu, 1983) for 1~2 weeks, rinsed with PBS, then incubated in biotinylated donkey anti-rabbit IgG (1:250; Jackson Immunoresearch) overnight, rinsed several times in PBS, and were processed according to the avidin-biotin-peroxidase complex (ABC) method using Vectastain ABC HRP kit (Vector Laboratories, Burlingame, CA, USA). After rinses in PBS, they were incubated in diaminobenzidine tetrahydrochloride (DAB) solution (Vector DAB substrate kit for peroxidase SK 4100) diluted with PBS for 5-15 min at room temperature. The sections were rinsed in PBS and then in PB, treated with 0.4% OsO_4 in 0.1 M PB for 1 hour at room temperature to enhance and stabilize the reaction products, and then dehydrated in graded series of ethanol, infiltrated in propylene oxide, and flat-embedded in Epon-Araldite. The stained sections were examined and recorded with a light microscope (Leica DM2500; Leica Microsystems, Tokyo, Japan) equipped with a digital camera (DS-Fi1; Nikon

Instech, Kawasaki, Japan). Some TH-positive cells were examined and drawn with a light microscope equipped with camera lucida apparatus at high magnifications using oil-immersion objective lens (Leica DM2500, Plan Apo 100 NA 1.40; Leica Microsystems, Tokyo, Japan).

For the multiple-fluorescent immunolabeling sections were incubated in the blocking/dilution solution overnight, then incubated in a mixture of primary antibodies such as chicken anti-TH (Aves; 1:2,500), rabbit anti-ankyrin G (AnkG, Santa Cruz SC28561; 1:500) and sheep anti-secretagogin (SCGN, BioVendor, RD184120100; 1: 5,000) for 4-14 days at 20°C. After rinsing in PBS the sections from wild type mice were incubated in a mixture of Alexa Fluor 488-conjugated donkey anti-chicken IgY (1:250; Jackson Immunoresearch, West Grove, PA, USA), indocarbocyanine (Cy3)-conjugated anti-rabbit IgG (1:1,000), indodicarbocyanine (Cy5)-conjugated anti-sheep IgG (1:250), and 4',6-diamidino-2-phenylindole (DAPI;1 μg/ml; Dojindo, Kumamoto, Japan) for 12~24 hours at 20°C. In case of the sections from TH-GFP mice Alexa Fluor 488-conjugated donkey anti-chicken IgY was omitted from the mixture of secondary antibodies. The sections were mounted in the Vectashield (Vector, Burlingame. CA) and covered with a cover glass. The sections were examined with the Neurolucida image analysis system (MBF Bioscience) composed of a fluorescence microscope (Nikon Eclipse 80i), a monochrome CCD digital camera (Retiga EXi; QImaging), motorized

digital imaging head (Nikon DIH-E) and motor-driven stage and focus drive (Ludl Electronic Products Ltd.). Fluorescent filter sets used were as follows; Semrock DAPI-1160B for DAPI and pacific blue, Semrock GFP-3035D for Alexa Fluor 488, FITC and GFP, Semrock TRIC-B for Cy3 and rhodamine red, Semrock Cy5-4040C for Cy5 and Semrock Lucifer Yellow B for LY. The sections were also observed under a confocal laser-scanning microscope (CLSM; TCS-SP2; Leica Microsystems, Vienna, Austria). Single laser beams, 405, 488, 564 and 647 nm in wavelength, were alternately used to collect images for different fluorescent signals. After acquiring the image stacks the same sections were processed for the ABC method: that is, the sections were incubated in 3% H_2O_2 in 80% methanol, then in chicken anti-TH (Aves; 1:5,000) overnight, then in biotinylated donkey anti-chicken IgY (1:500; Jackson Immunoresearch, West Grove, PA, USA) for 2-3hrs, followed by the incubation in the ABC complex (1: 500).

2-2. Glutamic acid decarboxylase (GAD) isoform, GAD67 and 65, immunolabelings and labeling intensity analysis

As is well known the detergent treatment such as Triton X 100 reduced the immunoreactivity for GADs in somata, which we also confirmed in the present study. Thus we prepared and analyzed the samples without detergent treatments. Several 50 μm thick sections were processed in Triton X-100 free solutions; sections were incubated in a mixture of 3 primary antibodies, that is, mouse anti-GAD67 (1: 5,000;

Chemicon, MAB5406, clone 1G10.2), rabbit anti-GAD65 (1: 10,000; Sigma G5038), and sheep anti-TH (1: 10,000; Chemicon, AB1542), and then, after rinsing several times in PBS, incubated in a mixture of donkey secondary antibodies, Cy3-conjugated anti-mouse IgG, Alexa Fluor 488-conjugated anti-rabbit IgG andCy5-conjugated anti-goat IgG (which cross-reacted with sheep IgG). After rinsing several times in PBS, the sections were mounted in the Vectashield. Image stacks were obtained near the section surfaces with the CLSM (Plan Apo CS oil x63 objective NA 1.32) or the Neurolucida system (PlanApo oil x100 objective NA 1.40). At the acquisition of image stacks the gain of each channel was adjusted at which few profiles were saturated. The image stacks obtained with the CLSM were analyzed by the Leica software AFS lite. The image stacks obtained with the Neurolucida system were analyzed by Image J 1.48v; the GAD65, GAD67 and TH channel stacks as well as their color-merged stacks were opened and synchronized with the plugin module SynchWindows. In both cases the somata which were supposed to be cut near their maximum diameters were selected, then we applied the best fitting ellipse to each selected somatic profile and obtained the areas of these ellipses. Then a small ellipse was overlaid on a part of each perikaryon of immunolabeled cells in an appropriate optical section in the stack, and the mean grey levels of each soma in 3 individual channels were measured. The relative immunolabeling intensities of GAD67 and GAD65 in individual TH positive neurons

were analyzed with the Microsoft Excel.

2-3. Tracer, biotinylated dextramine (BDA), labeling

In these experiments we used 37 C57BL/6J mice (24 male and 13 female mice), 6 weeks~7 months old 16-39 g (Japan SLC, Inc.) and 27 TH-GFP mice (12 male and 15 female mice), 6weeks~5 months old, 16~39 g. The animals were anesthetized with a mixture (0.1ml/10g body weight, intraperitoneal injection) of medetomidine hydrochloride (Domitor, Zenoaq; final concentration 0.03 mg/ml in physiological saline), midazolam (Sandoz; final concentration 0.4 mg/ml) and butorphanol tartrate (Vetorphale, Meiji Seika Pharma; final concentration 0.5 mg/ml), and then were mounted on a stereotaxic frame (SRS-A, Narishige Scientific Instrument Lab.). Through the glass microelectrodes with outside tip-diameters ranging from 10–20 μm, biotinylated 10 kDa dextran amine (2.5 % or 5% in physiological saline; BDA-10K, Molecular Probes) was injected iontophoretically by passing positive current (2-5 μA, 1 Hz, 20 % duty cycle) for 5-10 minutes into the GL of the medial part of each MOB. The micropipette tips were positioned 0.45-0.5 mm lateral from the midline at 10° over the MOB surface and inserted 1.2-1.3 mm from the surface into the GL of the medial side of the ipsilateral MOB. After the stereotaxic procedures atipamezole hydrochloride (Antisedan, Zenoaq; final concentration 0.075mg/ml, 0.1ml/10g body weight) was administered to the mice. After a survival period of 5-10 days mice were perfusion-

fixed. The brains were cut horizontally into 50 or 80 μm-thick serial sections on a vibratome (Leica VT1000S).

Sections were incubated in the blocking/dilution solution overnight, then incubated in Cy3-conjugated streptavidin (1:1,000; Jackson Immunoresearch) overnight at 20°C. The sections were examined with a fluorescent microscope. The series of sections containing appropriately BDA-labeled neurons were processed for multiple-fluorescent immunolabeling. The sections were incubated in a mixture of primary antibodies containing chicken anti-TH (1:2,500) and either sheep anti- SCGN (1:5,000) or rabbit anti-AnkG (1:500~1,000) for 4-14 days at 20°C. Then the sections from wild type mice were incubated in a mixture of Cy3-conjugated streptavidin (1:1,000), Alexa Fluor 488-conjugated donkey anti-chicken IgY (1:250), either Cy5-conjugated anti-rabbit IgG (1:250) or Cy5-conjugated anti-goat IgG (1:250), and 4',6-diamidino-2-phenylindole (DAPI;1 μg/ml; Sigma, St. Louis, MO, USA) for 12~24 hours at 20°C. In case of the sections from TH-GFP mice Alexa Fluor 488-conjugated donkey anti-chicken IgY was omitted from the mixture of secondary antibodies. Image stacks of multiple-fluorescent immunolabeled sections were obtained with the Neurolucida system. After acquiring the image stacks the same sections were processed for the ABC method: that is, the sections were incubated in 3% H_2O_2 in 80% methanol, then in biotinylated HRP (reagent B in Vectastain ABC HRP kit, 1: 250) overnight, followed by the incubation in

the ABC complex (1: 250).

2-4. Tracer, cholera toxin B (CTB), labeling

In these experiments we used 9 male C57BL/6J mice, 7weeks~5 months old 22-37 g (Japan SLC, Inc.). The animals were anesthetized and mounted on a stereotaxic frame as described above. The injection procedures were same to the BDA labeling. Instead of BDA cholera toxin B subunit (0.5% in 0.1N PB; CTB, low-salt cholera toxin B subunit, List Biological Laboratories, Campbell, CA) was injected iontophoretically by passing positive current (4 μA, 1 Hz, 10 % duty cycle) for 10 minutes into the GL of the medial side of the MOB. After a survival period of 7 days mice were perfusion-fixed. The brains were cut horizontally into 50 μm-thick serial sections on a vibratome (Leica VT1000S). Sections were incubated in the blocking/dilution solution overnight, then incubated in a mixture of primary antibodies containing goat anti-CTB (1: 5000; List Biological Labs, Inc), rabbit anti-TH (1:10,000; Nagatsu, 1983), guinea pig anti- VGluT2 (1:5,000; Frontier Institute Co. Ltd) and mouse anti-calbindin D28K (1: 20,000; Swant) for 4-14 days at 20°C and then, after rinsing several times in PBS, incubated in donkey biotinylated anti-goat IgG (1: 250, Jackson Immunoresearch) overnight at 20°C. Then, after rinsing several times in PBS, the sections were incubated a mixture of Pacific Blue-conjugated streptavidin (1:250, Molecular Probes), donkey FITC-conjugated anti-rabbit IgG (1: 250, Jackson Immunoresearch), rhodamine red-conjugated anti-guinea

pig IgG (1: 250, Jackson Immunoresearch) and Cy5-conjugated anti-mouse IgG (1: 100, Jackson Immunoresearch). After rinsing several times in PBS, the sections were mounted in the Vectashield. Image stacks were obtained with the CLSM.

2-5. Functional olfactory deprivation: unilateral nostril closure

In these experiments we used 36 C57BL/6J mice (31 male and 5 female mice: Japan SLC, Inc.). One nostril of mice, 4-8 weeks old 15-25g, was surgically closed using a spark-gap cautery (Morita PROG V) and sutured under the anesthesia with a mixture of medetomidine hydrochloride, midazolam and butorphanol tartrate. After 3-5 weeks mice were perfusion-fixed and 50 μm-thick serial sections were prepared as described above. Most sections were incubated in rabbit anti-TH (1: 100,000) for 1-2 weeks, and processed according to the ABC method.

Some sections were processed for multiple-fluorescent immunolabeling. After incubating in the blocking solution, the sections were incubated in a mixture of primary antibodies containing chicken anti-TH (1:2,500), rabbit anti- AnkG (1:500) and goat anti-olfactory marker protein (OMP 1:2500, gift from Dr. Margolis, Farbman and Margolis, 1980) for 4-14 days at 20°C. Then the sections were incubated in a mixture of Alexa Fluor 488-conjugated donkey anti-chicken IgY (1:250), Cy3-conjugated anti-rabbit IgG (1:250), Cy5-conjugated anti-goat IgG (1:250) and DAPI (1 μg/ml) for 12-24 hours at 20°C. Image stacks of multiple-fluorescent immunolabeled sections were

obtained with the Neurolucida system and then the same sections were processed for the ABC method as described above

2-6. Lucifer yellow (LY) labeling in fixed slices from TH-GFP mouse OBs

In this study we used 31 TH-GFP mice (19 male and 12 female mice), 4-8weeks old 15-25g. Mice were deeply anesthetized with sodium pentobarbital (100 mg/kg) and perfused transcardially with PBS (pH 7.4) followed by freshly prepared 4% paraformaldehyde in 0.1 M PB (pH 7.4). The brains were left in situ for 1-2 hours at room temperature, then removed from the skull and stocked for 2-4 hours in the same fixative at 7°C. The rostral parts of the brains were dissected out, encapsulated in 4 % agar in PBS and cut horizontally or parasagittally into 150 µm-thick sections on a vibratome (Leica VT1000S). Slices were transferred on a thin magnetic sheet (ca. 15x15 mm) glued to a Petri dish and then overlaid with a trimmed thin stainless steel plate with a slot. Under a fixed stage upright fluorescent microscope (Olympus BX50WI) GFP positive cells were penetrated with glass microelectrodes filled with 3 % Lucifer Yellow CH (dilithium salt; Sigma) in distilled water, and LY was injected by passing 2-20 nA negative current in 100 ms pulses applied at 1 HZ for 1-3 min. Then the slices were re-fixed in 4% paraformaldehyde in 0.1 M PB. Some slices were incubated in (DAPI (1 µg/ml) in PBS for 2-10 hours and image stacks were obtained with the Neurolucida image analysis system. Image stacks of 3 channels (DAPI, GFP, and LY)

were obtained using an objective lens x20 or x40. Most sections were processed for fluorescent multiple-immunolabeling. The LY injected slices were incubated in 3% H_2O_2 in 80% methanol for 2hours (to bleach GFP), rinsed with PBS, then incubated in blocking/dilution solution overnight, incubated in a mixture of primary antibodies, chicken anti-TH (1:2500), guinea pig anti-LY (our own antibody; 1:10000) and rabbit anti-AnkG (1:500) for 4-14 days, then incubated in a mixture of DAPI and fluorochrome-conjugated secondary antibodies raised in donkeys (Jackson Immunoresearch), rhodamine red-conjugated anti-chicken IgY (1:250), Alexa Fluor 488-conjugated anti-guinea pig IgG (1:500), Cy5-conjugated anti-rabbit IgG (1:250) for 12~24 hours. The sections were mounted in the Vectashield (Vector, Burlingame. CA) and covered with a cover glass. The sections were examined with a Neurolucida image analysis system. Image stacks of 5 channels (DAPI, Alexa Fluor 488, rhodamine red, cy5 and LY) were obtained using an objective lens x20 or x40. By adjusting the camera setting the somata and thick processes of LY-labeled neurons were observed in the LY channel and their thin processes in the Alexa Fluor 488 channel; at that camera setting the thin processes were barely visible in the LY channel and on the other hand somata and thick processes were obscured by bright halos in Alexa Fluor 488 channel. The guinea pig anti-LY used in this study was raised against keyhole limpet hemocyanin-conjugated LY VS. No stainings were encountered in control sections.

2-7. Biocytin labeling in live slices from TH-GFP mouse OBs

For these experiments we used a transgenic mice strain (TH-GFP/21–31), carrying the eGFP transgene under the control of the TH promoter (Sawamoto et al., 2001; Matsushita et al., 2002); for biocytin labeling we used 23 mice (8 males and 15 females), 3 weeks~7 months old. The TH-GFP strain was maintained as heterozygous by breeding with C57BL/6J inbred mice.

For the dissection and slice preparation, a high sucrose artificial cerebrospinal fluid (ACSF) solution was used with the following composition (in mM): 215 sucrose, 3 KCl, 21 $NaHCO_3$, 1.25 NaH_2PO_4, 1.6 $CaCl_2$, 2 $MgCl_2$, and 10 glucose. For electrophysiological biocytin injection experiments, a standard extracellular solution was used with the following composition (in mM): 125 NaCl, 2.5 KCl, 26 $NaHCO_3$, 1.25 NaH_2PO_4, 2 $CaCl_2$, 1 $MgCl_2$, and 15 glucose. The osmolarity of external solutions was adjusted at 305 mOsm with glucose and solution was continuously bubbled with 95% O_2 and 5% CO_2 during the experiment. The pipette-filling intracellular solution with biocytin contained (in mM): 120 KCl, 10 NaCl, 2 $MgCl_2$, 0.5 $CaCl_2$, 5 ethylene glycol tetraacetic acid (EGTA), 10 HEPES, 2 Na-ATP, 10 glucose and 0.5-1 % biocytin hydrochloride (Sigma) was added. The osmolarity of intracellular solution was adjusted to 295 mOsm with glucose, and the pH to 7.2 with KOH. The free calcium concentration was calculated to be 16 nM.

The surgical procedures were described previously (Pignatelli et al., 2009). Slices (350 µm thickness) in the coronal or sagittal plane were obtained using a Campden 752 vibroslice tissue cutter (Campden Ltd., Loughborough, England). Electrophysiological recordings were acquired with a Multi-Clamp 700B amplifier (Molecular Devices, Sunnyvale, CA, USA), and a 12 bit A/D–D/A converter (Digidata 1440A; Molecular Devices). Borosilicate glass pipettes (1.5 O.D., 0.87 I.D., with filament; Hilgenberg,

Malsfeld, Germany) were pulled with a Sutter P-97 puller (Novato, CA, USA) and had a resistance of 4–5 MΩ when filled with intracellular byocitin solution; the seal formation was realized with the help of an air pressure controller (MPI, Lorenz Messgerätebau, Katlenburg-Lindau, Germany); the seal resistance was always greater than 2 GΩ.

During the experiment, the 1-ml recording chamber was constantly perfused with an approximately 2 ml/min flux of extracellular solution. Slices were covered by a homemade grid in inert material to avoid vibrations and folding of the preparation during the recordings. An upright microscope Olympus BX50WI equipped with Nomarski differential interference contrast (DIC) optics and epifluorescence was used in order to identify eGFP-expressing cells in the preparation.

Only the cells with an access resistance below 30 MΩ were used for the experiment and the biocytin was allowed to penetrate for 10-15 minutes.

After biocytin injections the slices were immersion fixed in 4% paraformaldehyde in 0.1 M PB. The slices were processed for fluorescent multiple-immunolabeling; slices were incubated in the blocking/dilution solution overnight at 20°C, incubated in chicken anti-TH (1; 2,000) for 1-2weeks, and then after rinses in PBS incubated in a mixture of Cy3-conjugated streptavidin (1: 500), FITC-conjugated donkey anti-chicken IgY (1: 200) and DAPI (1 μg/ml) or a mixture of pacific blue-conjugated streptavidin (1: 200), FITC-conjugated donkey anti-chicken IgY (1: 200) and propidium iodide (5μg/ml) overnight. The slices were mounted in the Vectashield and covered with a cover glass. To prevent the compression of the slices we mounted a 300μm-thick agar sheet, ca. 10x10 mm, with a hole, 5mm in diameter, on the glass slide, and each slice was located in the hole. The observations with a confocal laser-scanning microscope (CLSM) were described as above. After observations and recordings some slices were processed for the ABC method; the slices were incubated in 3% H_2O_2 in 80% methanol overnight,

then in biotinylated HRP (reagent B in Vectastain ABC HRP kit, 1: 250) overnight, followed by the incubation in the ABC complex (1: 250) for 5-7 hours. After rinses in PBS, they were incubated in DAB (Vector DAB substrate kit for peroxidase SK 4100), rinsed in PBS and mounted in an aqueous mounting medium Aquatex (Merk). Some slices processed for ABC method were embedded in gelatin, cut into 50 μm thick serial sections with a vibratome, flat mounted on glass slides, air dried, covered with 0.04 % OsO4 in a moisture chamber, rinsed with MilliQ water, dehydrated in graded series of ethanol and embedded in Epon-Araldite.

3. Results

In the present study we used four methods to reveal the structural features of TH expressing neurons, especially JG ones; BDA labeling, functional olfactory deprivation, LY injection in fixed slices and biocytin injection in live slices. These methods appeared to be rather complementary to one another. However, before describing the structural features we had better point out the problem of tissue shrinkage. Several neurons fluorescently labeled and recorded were further processed for ABC-DAB methods. The processing of ABC-DAB methods induced some shrinkage of the fluorescently labeled samples. By comparing the fluorescent and brightfield images of individual neurons directly, the cells in the brightfield images were revealed to shrink to about 90 % (88.1 ± 5.9 %, N=17 neurons) of the fluorescent images in length. Thus in the present study we applied the shrinkage correction (1.1 = 1/0.9) to

the brighfield images to compare the images obtained with various methods.

In the MOBs TH expressing neurons were clustered in the GL, but they were also scattered in other layers (Fig. 1 A). In the GL TH expressing somata were clustered around the glomeruli which were occupied by numerous positive processes. The TH expressing somata around the glomeruli were apparently heterogeneous in their sizes (Fig. 1 B). In the present report we mainly described the structural features of the TH expressing neurons in the GL and the adjacent regions, and described those in the other layers rather briefly.

3-1. Cells in the GL

3-1-1. GAD65 & GAD67 localization

In the MOBs PG cells were reported to be strongly labeled for two GADs (Esclapez et al. 1994). On the other hand recent analyses on transgenic mice, GAD65-GFP mice (Parrish-Aungst et al.. 2007) and GAD67-GFP mice (Kiyokage et al., 2010), reported that TH expressing JG cells rarely coexpress GAD65. Thus we examined the immunointensities of GAD isoforms in individual TH immunopositive neurons of wild type mice, especially the relationship between the soma sizes and immunointensities of GAD isoforms. In the JG region GAD67 positive somata apparently outnumbered GAD65 positive somata. All GAD65 positive somata in the JG region were confirmed to be GAD67 positive, so far examined. Most of small~medium sized TH positive JG cells

were both GAD65 and GAD67 positive, although the larger type of TH positive JG cells were usually only faintly GAD65 positive or nearly GAD65 negative (Fig. 2 A-D). The analysis of the intensities of GAD65 and GAD67 immunoreactivities of individual TH positive JG cells (Fig. 3 A-D) showed that the large ones (e.g. in the case shown in Fig. 3, more than 12 μm in diameter) displayed the faint GAD65 immunoreactivity and the low level of GAD65/GAD67 grey level ratio (Fig. 3 B, D).

3-1-2. Soma sizes and axonal processes with the AIS marker

As reported previously (Pignatelli et al., 2005; Kosaka and Kosaka, 2008b), TH expressing JG neurons were classified into at least two groups on the basis of their soma sizes. In the case shown in Fig. 4, the soma size distribution was fitted with two normal distributions, that is, the peak and half width of the diameters of the smaller group were 9.9 and 2.5 μm, and those of the larger group 13.8 and 2.1 μm, respectively, in the case shown in Fig. 4 C. As we discussed previously (Kosaka and Kosaka, 2016) the larger type of TH expressing JG neurons have the typical axonal processes with the AIS markers such as Ankyrin G (Fig. 4 A, B), whereas almost of the smaller type have no such processes. Fig. 4 shows clearly the relationship between the soma sizes and the presence of AnkG positive processes, indicating that the TH positive JG neurons with AnkG positive processes consisted of a single population in their soma sizes (diameter ±

SD = 14.1 ± 1.5 μm) and corresponded well to the larger type. As described in detail later, these typical axons arising from large somata extended to numerous glomeruli located not only near their somata but also far from their somata. On the other hand almost of the smaller type of TH positive JG neurons appeared to be lack of the AnkG positive processes. However we must consider the following three points here. First we encountered, although rarely, small~medium sized TH positive JG neurons with faintly AnkG positive thin processes. Second AnkG negative thin processes which were morphologically presumed to be axons were occasionally encountered, indicating that there might be axons without the detectable levels of the AIS molecular markers. Third, fluorescently unrecognized thin axonal processes were sometimes revealed after the ABC-DAB processing, indicating that at least some of fluorescently anaxonic neurons could be axonic when examined with more sensitive methods, although they did not show the AIS molecular markers, so far examined.

3-1-3. neuron types

In the control/nondeprived MOBs TH-immunopositive/TH-GFP-positive processes were compactly packed and intermingled with one another in glomeruli and thus traced only outside the glomeruli and/or near the peripheral portions of the glomeruli; in glomeruli those individual processes were nearly impossible to be traced

(Figs. 1, 5, 6). On the other hand in functionally deprived MOBs the TH-immunopositive neurons decreased in number, and thus the intraglomerular TH-immunopositive processes were decreased, which occasionally made possible to trace the remaining TH-immunopositive individual neurons and their processes even in glomeruli (Figs. 5, 6, 8). The structural features of TH-immunopositive individual neurons encountered in the deprived MOBs corresponded rather well to those observed in the non-deprived control MOBs revealed by in vivo BDA labelling, LY-labeling in fixed slices and biocytin-labeling in in vitro live slices (Figs. 5, 6, 8-10). Thus the structural features of TH immonopositive neurons in the functionally deprived MOBs were presumed to represent those in the normal MOBs, at least to some extent. In the present paper we described the structural features of TH expressing neurons obtained with various methods collectively.

In the glomerular region we recognized at least 4 types of TH expressing JG neurons; that is, 1) large neurons with typical axons and tuft-like glomerular dendritic branches which we named previously as "inhibitory juxtaglomerular association neurons (IJGA neurons)", but we would like to name "large periglomerular cells, LPG cells" here based on their structural features described below (Figs. 5-7), 2) so-called periglomerular cells, which we would like to name "small periglomerular cells, SPG cells" (Fig. 8), 3) transglomerular cells (Fig. 9) extending dendritic processes spanning

several glomeruli and 4) small~medium sized cells extending dendritic processes in the periphery of glomeruli, which we would like to name "incrusting cells" here (Fig. 10). However, there were many other neurons which we could not classify into anyone of these 4 types and thus might be classified into another different types of JG cells (Fig. 11). In the present study we first described the structural features of 4 types of neurons, and then briefly the structural features of some representative ones of those yet-unclassified neurons.

3-1-3-1 Large neurons with typical axons: large periglomerular cells (LPG cells) or inhibitory juxtaglomerular association neurons (IJGA neurons)

In control MOBs large neurons with typical axons were easily recognized near the border between the GL and EPL. In multiple-fluorescent immunolabeled samples those axons usually displayed the ankyrinG (AnkG) immunoreactivity on their initial portions, axon initial segments (AISs) arising from the somata or thick dendrites. The dendritic processes in the GL were barely traced due to the intensely TH immunoreactive numerous elements in the glomeruli: several rather thick dendritic processes extended from the somata and their branches toward glomeruli and occasionally appeared to penetrate further into glomeruli (Figs. 5, 6). In deprived MOBs we also encountered large neurons with typical axons near the border between

the GL and EPL (Figs. 5, 6). In addition we also recognized similar type of neurons in the middle of the GL (Fig. 6 cells 6, 9) where a small number of TH immunoreactive neuronal somata and processes were scattered. In the deprived MOBs as well as BDA- or LY-labeled samples we could observe both dendritic processes and axons of those large TH expressing neurons far more in detail (Figs. 5, 6). Dendritic processes frequently made tufts in the GL. Some made a compact tuft in one glomerulus with a few branches outside that glomerulus (Fig. 5 cell 2, Fig. 6 cells 3, 12). Another made somewhat loose tufts spanning 2~4 glomeruli (Fig. 5 cell 3, Fig. 6 cells 7-10, 14). Another made two separate tuft-like clusters of dendritic branches in two different glomeruli (Fig. 6 cells 4-6, 13). Dendritic processes were rather smooth but bore a few spines. Axonal processes were traced in various length. By the combined multiple-fluorescent immunolabeling and ABC-DAB processing we traced the axonal processes identified with the AnkG positive AISs in serial sections (Fig. 5). The axons of the large TH expressing neurons were easily differentiated from dendritic processes (Figs. 5, 6), which then made us possible to trace the axonal processes without the AIS marker-labeling in many cases. Axons arose either from the somata or the thick dendritic shafts, and usually extended toward the ML, branched in the EPL and then extended laterally; axonal branches frequently further extended toward the GL and some were traced into the GL and into the glomeruli. However, we also encountered some neurons

whose axons extended laterally in the GL spanning several glomeruli (Fig. 6 cells 6, 7, 9). Interestingly we occasionally encountered neurons with 2 or 3 axons (Fig. 4 cell 1, Fig. 6 cells 2, 8, 9, 13). In the BDA labeling and LY labeling samples those large TH expressing neurons showed similar structural features described above but their axonal processes could be traced only near the somata and their intraglomerular dendrites appeared to bear more spines than those observed in the deprived MOBs.

To further confirm the axonal processes in the GL we applied a small amount of CTB, an anterograde and retrograde tracer, into the restricted region of the GL (Fig. 7). Near the injection sites CTB labeled rather diffusely the GL, EPL and lower layers (Fig. 7B). However in some distant regions, 200-1500 μm from the injection sites, retrogradely labeled somata were scattered mainly in the GL and upper EPL; the labeling was always restricted to the perikarya and so far we encountered no dendritic processes showing the Golgi-like CTB-labeling. Corresponding well to the data of our previous retrograde tracer fluorogold (FG) labeling study (Kosaka and Kosaka, 2008b), the majority of labeled somata were confirmed to be TH positive (Fig. 7A). In addition small labeled puncta or strings of puncta were scattered in the GL, some of which were also confirmed to be TH positive (Fig. 7A, C1-3). Interestingly most of those TH positive CTB labeled puncta were located in the VGluT2 positive regions in glomeruli, that is, the ON zone, indicating that axon terminals of the presumed LPG neurons mainly

distributed in the ON zone of the glomeruli.

3-1-3-2 Small periglomerular cells (SPG cells)

The TH expressing neurons with small~medium sized somata were clustered in the JG region and their processes were barely traced in the GL of the control MOBs as described previously: but in some cases relatively proximal portions of the processes arising from the somata were observed which branched in glomeruli (Fig. 1B). In BDA/biocytin/LY labeled samples and deprived MOBs the structural features of these neurons were displayed in detail (Fig. 8). Dendritic processes were usually spiny and somewhat varicose; 1~4 dendritic stems arose from the somata, making tufts. Some were uni-glomerular making one tuft in a glomerulus (Fig. 8 cells 1-4, 10-14, 16, 18, 19, 21, 22), whereas others were bi- or tri-glomerular making two or three tufts in nearby different glomeruli (Fig. 8 cells 5-7, 15, 17, 20, 23-25) In addition some displayed a few extraglomerular dendritic branches (Fig. 8 cells 8, 9). In the ABC-DAB samples thin processes with a few varicosities were sometimes observed to extend from the somata but were traced in rather short distances in the present samples (Fig. 8 cells 18-21), which appeared to be axons, although the majority of small~medium sized neurons appeared to have no such thin axonal processes. Those thin axon-like processes were rarely recognized in the fluorescent samples. However, in some cases "anaxonic" cells in

the fluorescent samples were turned out to be "axon-bearing" after the ABC-DAB processing, showing very thin faintly stained axonal processes. Cell 21 in Fig. 8 was an exceptional case which displayed two, although faintly, AnkG positive thin axonal processes extending from the soma.

3-1-3-3 Transglomerular cells

Transglomerular cells were found among SCGN positive JG neurons (Kosaka and Kosaka 2013). Among SCGN positive neurons some extended slender dendritic processes into a glomerulus which penetrated into another nearby glomeruli, spanning two or three glomeruli. Thus we named them “transglomerular cells (TG cells)." As described previously (Kosaka and Kosaka 2016), we indicated that there might be SCGN negative transglomerular cells. In the present study we encountered TH expressing transglomerular cells (Fig. 9). We confirmed that at least some of them were SCGN negative. TH expressing transglomerular cells closely resembled SCGN positive ones in their overall structural features. The medium-sized somata extended 2~4 dendritic processes in the GL more or less parallel to the layer, which usually bore relatively long irregular spines and spanned 2~3 glomeruli; so far we encountered dendritic processes spanned up to 6 glomeruli (Fig. 9 cell 4). Some and/or some parts of the dendritic processes occasionally located at the periphery of the glomeruli or

periglomerular regions, which made the border between the transglomerular cells and the incrusting cells described below somewhat vague.

3-1-3-4 Incrusting cells

In the present study we encountered TH expressing JG neurons extending more or less spiny dendritic processes mostly in the periphery of the glomeruli as well as in the periglomerular and/or subglomerular regions, appearing to incrust some parts of the glomeruli, although some dendritic processes were located near the center of the glomeruli (Fig. 10). Most cells apparently extended their dendritic branches into two or more different glomeruli. In the periglomerular and/or subglomerular regions, where somata clustered, their dendritic processes appeared to contact with somata in these regions. Taking the distribution of their dendritic processes into consideration, most of these neurons resembled "clasping cells" reported recently by Bywalez et al. (2017). However, we could not necessarily confirm the protrusions clasping somata or rather we encountered numerous dendritic spines which did not clasp any somata. Furthermore some cells apparently extended their dendritic branches into two different glomeruli. Thus we would like to call this type of cells as "incrusting cells" rather than "clasping cells". So far as we examined we encountered no cells of this type with axonal processes.

3-1-3-5 Other neurons

In the GL there were various types of TH immunopositive/TH-GFP positive neurons which were not necessarily classified into four types described above. Here we just displayed some of them (Fig. 11), which remain to be analyzed further in detail. Some cells extended their dendritic branches into several glomeruli (Fig. 11 cells 5-7), which could be named "oligoglomerular juxtaglomerular neurons" (but not "oligoglomerular short-axon cells" as they appeared to have no axonal processes). Cells 9-11 in Fig. 11 were confirmed to be TH positive and SCGN positive.

3-2. Cells located in the EPL, MCL, IPL and GCL

TH expressing neurons were clustered in the GL, but they were also scattered in other layers, which were apparently various in shapes and sizes (Figs. 1, 12, 13). Large neurons with apparent axons were scattered mainly in the superficial half of the EPL. Some of them extended thick cylindrical smooth dendrites laterally or upwards to the GL, which appeared to extend further into the GL. Those large neurons corresponded to the displaced LPG cells or displaced IJGA neurons (Fig. 12 cell 2). Some of other large neurons had dendritic processes extended both upwards to the GL and downward to the MCL~GCL (Fig. 12 cells 1, 3-5). Some other relatively large neurons appeared to be inverted pyramid in shape (Fig. 12 cells 6-8); they were located

in the upper half to middle one-third of the EPL or rather close to the border between the EPL and GL and they extended one or two thick dendrites toward the MCL whose branches were extended laterally in the MCL~IPL, on the other hand relatively short thin dendritic branches also extended from their somata and distributed in the border between the EPL and GL, and some extended further to the GL. Presumed axonal processes arising from these neurons were occasionally encountered. Among others with no apparent axonal processes, some also extended dendritic processes into the GL (Fig. 13A). In control MOBs those processes could be traced only near the border between the GL and EPL, but in deprived MOBs those processes were traced further into the GL where they branched and occasionally made small tuft-like structures (Fig. 13 cells 7-11).

In the EPL~GCL small TH expressing cells of various shapes were also scattered (Figs. 1A, 13B). Among them presumed displaced SPG cells were also encountered in the upper half of the EPL, which extended dendritic processes to the GL and formed tufts in the glomeruli (Fig. 13 cells 12, 18).

4. Discussion

The present study revealed the structural features of the TH expressing neurons in the mouse MOBs. Similar to previously reported chemically defined neurons in the MOBs such as CB, PV,

NOS and SCGN expressing neurons TH expressing neurons were also heterogeneous in their structural features.

4-1. GAD isoforms

In the present study we showed that the larger type of dopaminergic JG cells displayed the low level of GAD 65 immunoreactivity and low level of GAD65/GAD67 grey level ratio whereas the smaller type of dopaminergic JG cells showed the various levels of GAD 65 immunoreactivity (faint ~intense) and GAD65/GAD67 grey level ratio. Thus the smaller type of dopaminergic JG neurons are heterogeneous in the composition of their GAD isoforms, whereas the larger type might be rather homogeneous. Regarding with GAD isoform expressions in dopaminergic JG cells, Parrish-Aungst et al. (2007) reported that "6.85 % of TH cells express only GAD65-GFP, 12.15 % express both GAD65-GFP and GAD67, 58.85 % express only GAD 67 and 22.35 % express only TH." In their analysis, Parrish-Aungst et al. (2007) added the detergent Triton X to the incubation media, which was supposed to decrease significantly the somatic immunolabeling for GAD67. Furthermore judging from their figures showing the relationship between TH and GAD65-GFP (Figs. 3, 4 in Parrish-Aungst et al., 2007), the percentage of TH neurons coexpressing GAD65-GFP appears to be much higher than 20 %; that is, approximately 75% of TH+ cells (for example, 32 TH+ GAD65-GFP+/42 TH+ in Fig. 3C in Parrish-Aungst et al., 2007), although we could not evaluate exactly the z-axis resolution from the figures displayed. This value of

the percentage of GAD65+ TH expressing JG cells we estimated from their figures, 75%, appears to correspond well to the value deduced from Fig. 3 in the present paper: among 134 TH positive JG cells 97 cells (72 %) showed the GAD65 grey level above 50, the value confidently recognized as positive. On the other hand Kiyokage et al. (2010) reported that "Immunostaining for TH in GAD67-GFP mice showed that virtually all (97.4 ± 1.2%) TH+ cells coexpress GAD67 (n = 4 animals, 233 TH+ cells), with 18% also expressing GAD65 (Parrish-Aungst et al., 2007)." Furthermore Kiyokage et al (2010) concluded that "the GAD65+ and TH+ chemotypes comprise predominantly nonoverlapping populations of JG cells. GAD65+ cells are purely GABAergic, and TH+GAD67+ cells are DA-GABAergic." However, considering the heterogeneity of dopaminergic JG cells and the relatively intense GAD65 expression in most of smaller type of dopaminergic JG cells into consideration, their conclusion must be oversimplified and misleading.

4-2. Cells in the GL: morphological & chemical properties.

Dopaminergic small periglomerular (SPG) cells shown in the present study corresponded very well to those classical PG cells, or outer granule cells, identified with Golgi impregnation methods (Figs. 414-416 of Ramon y Cajal 1995); "Their *perikarya* give rise to one or more thin *dendrites* that arborize within the depths or periphery of the glomeruli. In addition, they give rise to a very thin *axon* that courses more or less

tangentially between glomeruli and then ends by ramifying within one of them. …. Blanes distinguished *uni-* and *biglomerular granule cells* based on whether their dendrites enter one or two glomeruli (Figs. 414, 415, 416). It would appear from this description that the small intra- and periglomerular cells (Kölliker's outer granule cells) constitute association neurons between glomeruli (Ramon y Cajal 1995)." It is important to note that classical PG cells are not necessarily uni-glomerular but some are bi- or, as we showed, tri-glomerular. In some previous reports (Kiyokage et al. 2010, Bywalez et al. 2017) PG cells were concluded not to belong to dopaminergic neurons. However our present study as well as a previous study of another research group (Galliano et al. 2018) clearly showed that there are dopaminergic small PG cells. This discrepancy in the presence of dopaminergic PG cells among these reports might be caused by the differences in the methods used and the definition of PG cells. Interestingly Kiyokage et al. (2017) examined the synaptic connections of small dopaminergic JG neurons with the electron microscopic serial section-reconstruction; the neurons reconstructed were shown to extend their dendrites into glomeruli and receive numerous asymmetrical synapses from ON terminals, M/T dendrites and non-ON terminals and a few symmetrical synapses from presumed GABAergic processes and make symmetrical synapses mainly to M/T dendrites. These features appears to correspond to those of PG cells, especially "type 1 PG cells" as suggested in their paper

(Kiyokage et al. 2017), although the authors used just the term "TH-expressing JG cells" instead of PG cells and short-axon cells. In the present study we could not confirm the axonic processes in most SPG cells, but we encountered a few dopaminergic SPG cells displaying thin axonic processes although almost of them were AnkG negative. There might be both axonic and anaxonic dopaminergic SPG cells; the former might correspond to the classical PG cells.

In the present study we revealed the structural features of the larger type of dopaminergic JG cells. They displayed dendritic processes located in one to several glomeruli usually making tufts and apparent axonal processes extending rather distantly as well as near their somata and penetrating into glomeruli. The overall structural features might correspond well to those of classical PG cells described above but their larger sizes. Thus we would like to name them "large periglomerular cells LPG cells", whereas the smaller type of PG cells, both axonic and anaxonic ones, might be named "small periglomerular cells SPG cells." Furthermore it seems comprehensible that these LPG cells could be regarded as "external tufted cells" if we had not known their GABAergic nature.

Most of the dopaminergic JG neurons with AIS shown in Fig. 3 of their paper by Galliano et al. (2018) might correspond to the LPG cells. In addition DA-GABAergic polyglomerular short-axon cells shown in Fig. 6 of their paper by Kiyokage et al. (2010)

might also correspond to the LPG cells, when we regard short processes near the somata as dendrites and distantly extending processes as axons. At any rate the extent of the dendritic field of the LPG cells or so-called "polyglomerular short-axon cells" might be not polyglomerular but rather oligoglomerular. Furthermore, these LPG cells and axonic SPG cells are so-called short-axon cells in general term (Nagayama et al. 2014) but we prefer not to apply the term "short-axon cells" to these neurons in the OBs, as we discussed previously in detail (Kosaka and Kosaka, 2016). In addition, as we reported previously, there are some types of genuine "superficial short- axon cells (Pinching and Powell 1971)" in the MOBs, that is, NOS positive superficial short- axon cells (Kosaka and Kosaka, 2007), PV positive superficial short- axon cells (Kosaka and Kosaka, 2008a) and CB positive superficial short- axon cells (Kosaka and Kosaka, 2010).

We encountered dopaminergic JG cells displaying the structural features of transglomerular cells. Transglomerular cells were previously shown in our study on secretagogin (SCGN) positive JG cells in the mouse MOB (Kosaka and Kosaka, 2013), which extended slender dendritic processes into a glomerulus which penetrated into another nearby glomeruli, spanning two or three glomeruli. Dopaminergic transglomerular cells shown in the present study resembled SCGN -containing transglomerular cells in their structural features. However, dopaminergic

transglomerular cells were confirmed to be different from SCGN positive transglomerular cells. Furthermore we also encountered transglomerular cells which were neither dopaminergic nor SCGN positive, indicating that transglomerular cells consist of heterogeneous groups of neurons in their chemical properties, although it remains to be revealed whether or not there are some, even subtle, structural differences among chemically different transglomerular cells. These transglomerular cells resembled some of the so-called "oligoglomerular short-axon cells (Kiyokage et al. 2010). However, we observed no axonal processes arising from transglomerular cells so far examined, and thus we also prefer not to use "oligoglomerular short-axon cells."

As described in the Result section the incrusting cells somewhat resembled "clasping cells CCs" reported recently by Bywalez et al. (2017). Clasping cells were defined by several characteristics of their dendritic processes: dense dendritic arborizations clasping around other JG somata, dendrites mostly ramifying in the JG space of the GL, and no dendritic branches in the EPL. In addition, Bywalez et al. (2017) described as follows; "If these dendrites ever entered the glomerular neuropil (in 8 out of 16 fully reconstructed cells with parent glomerulus), they did so only in a restricted fashion, namely within mostly superficial volumes of one particular glomerulus. No substantial projection into any additional glomeruli was observed." Thus the incrusting cells we named in the present study resembled the clasping cells in

overall structural features. The clasping cells might be considered as a particular subtype of the incrusting cells. Bywalez et al. (2017) considered that their clasping cells corresponded to "oligoglomerular short-axon cells" reported by Kiyokage et al. (2010), speculating that "the extended oligoglomerular innervation might be performed by the CC's axon (which is lacking from our reconstructions), while the dendrites project mostly into the juxtaglomerular space (Bywalez et al., 2017).", although the axons of clasping cells were not yet stained. However, the "oligoglomerular short-axon cells" of Kiyokage et al. (2010) appeared to be heterogeneous in their structural features judging from their Fig. 5 B; some appeared to be anaxonic and resembled the transglomerular cells as described above, whereas the cell shown in the lower left corner appeared to have an axonal process innervating several adjacent glomeruli. Presumably it is important to reveal the axonal processes, if present, of clasping cells and oligoglomerular short-axon cells to determine whether they are the same or different types of cells. Furthermore according to the description in the text of Ramon y Cajal (1995) on the PG cells "Their *perikarya* give rise to one or more thin *dendrites* that arborize within the depths or periphery of the glomeruli. …", the incrusting cells extending their dendritic processes in the periphery of glomeruli might be regarded as a subtype of PG cells. In the present study we encountered some dopaminergic JG neurons extending their dendrites into the center of a glomerulus and another to the

periphery of another glomerulus (Fig. 11 cell 8), which might be included either into incrusting cells or SPG cells or unclassified cells. We previously reported SCGN expressing neurons in the mouse MOBs (Kosaka and Kosaka, 2013). In addition to the transglomerular cells some of SCGN expressing neurons (e.g. cells 8, 9, 12 in Fig. 17A in Kosaka and Kosaka, 2013) resemble dopaminergic incrusting cells or unclassified JG neurons shown in the present study. There might be various types of neurons with similar structural features but chemically different properties.

4-3. Cells in the EPL~GCL

Liberia et al. (2012) reported the details of TH immunopositive cells in the EPL of the rat MOBs at the light and electron microscopic levels. TH expressing cells in the EPL of the mouse MOBs resembled those of the rat MOBs in their structural features and thus it might be unnecessary to discuss in detail here. We would like to point out just one issue. In addition to apparent displaced LPG cells and SPG cells, we encountered some TH expressing cells in the EPL extending their dendritic processes into the GL and, in the deprived MOBs, we observed some of those dendritic processes making small tufts in the GL. These observations correspond well to the previous physiological observations that some EPL dopaminergic neurons responded monosynaptically to the ON stimulation (Pignatelli et al., 2009). Various types of dopaminergic neurons other than JG ones might participate in the glomerular neuropil.

4-4. Concluding remark

As described in the Introduction, DA-GABAergic JG neurons are supposed to play important roles in the control of glomerular outputs in the MOBs (Banerjee et al., 2015; Liu et al., 2016; Vaaga et al., 2017; Shao et al., 2019: for review, Pignatelli and Belluzzi, 2017; Burton, 2017). However, the present study revealed the heterogeneity of the DA-GABAergic JG neurons. At present we know almost nothing about the synaptic connections of each type of DA-GABAergic JG neurons. Recent reconstruction study on the presumed SPG cells (Kiyokage et al. 2017) revealed the synaptic connections of this type of DA-GABAergic JG neurons to some extent and thus leaded to some functional implications of SPG cells. Similar detailed analyses on each type of DA-GABAergic JG neurons are necessary before we discuss the functional importance of each type of DA-GABAergic JG neurons.

Funding: This work was supported by JSPS KAKENHI Grant 17K08519, Research funds from IUHW and Research funds from University of Ferrara.

Conflict of Interest: The authors declare there are no known conflicts of interest associated with this publication

.

Author contributions: T. K designed the research; T. K., A. P, and K. K. performed research, analyzed data and wrote the paper.

Acknowledgements

The authors thank Drs. I. Nagatsu and F. Margolis for their gifts of primary antibodies. The authors also thank Drs. O. Belluzzi and Alex Fogli Iseppe for their help in live slice experiments.

References

Banerjee, A., Marbach, F., Anselmi, F., Koh, M.S., Davis, M.B., Garcia da Silva, P., Delevich, K., Oyibo, H.K., Gupta, P., Li, B., Albeanu, D.F., 2015. An interglomerular circuit gates glomerular output and implements gain control in the mouse olfactory bulb. Neuron 87, 193-207.

Burton, S.D., 2017. Inhibitory circuits of the mammalian main olfactory bulb. J. Neurophysiol. 118, 2034-2051.

Bywalez, W.G., Ona-Jodar, T., Lukas, M., Ninkovic, J., Egger, V., 2017. Dendritic arborization patterns of small juxtaglomerular cell subtypes within the rodent olfactory bulb. Front. Neuroanat. 10, 127. DOI: https://doi.org/10.3389/fnana.2016.00127.

Davis, B.J., Macrides, F., 1983. Tyrosine hydroxylase immunoreactive neurons and fibers in the olfactory system of the hamster. J. Comp. Neurol. 214, 427–40.

Esclapez, M., Tillakaratne, N.J.K., Kaufman, D.L., Tobin, A.J., Houser, C.R., 1994. Comparative localization of two forms of glutamic acid decarboxylase and their mRNAs in rat brain supports the concept of functional differences between the forms. J. Neurosci. 14, 1834-1855.

Farbman, A., Margolis, F., 1980. Olfactory marker protein during ontogeny: Immunohistochemical localization. Devl. Biol. 74, 205-215.

Gall, C.M., Hendry, S.H.C., Seroogy, K.B., Jones, E.G., Haycock, J.W., 1987. Evidence for coexistence of GABA and dopamine in neurons of the rat olfactory bulb. J. Comp. Neurol. 266, 307–318.

Galliano, E., Franzoni, E., Breton, M., Chand, A.N., Byrne, D.J., Murthy, V.N., Grubb, M.S., 2018. Embryonic and postnatal neurogenesis produce functionally distinct subclasses of dopaminergic neuron. eLIFE 7, e32373. DOI: https://doi.org/10.7554/eLife.32373.

Halász, N., Johansson, O., Hökfelt, T., Ljungdahl, Å, Goldstein, M., 1981. Immunohistochemical identification of two types of dopamine neuron in the rat olfactory bulbs as seen by serial sectioning. J. Neurocytol. 10, 251-259.

Kiyokage, E., Kobayashi, K., Toida, K., 2017. Spatial distribution of synapses on tyrosine hydroxylase-expressing juxtaglomerular cells in the mouse olfactory glomerulus. J. Comp. Neurol. 525, 1059-1074.

Kiyokage, E., Pan, Y.Z., Shao, Z., Kobayashi, K., Szabo, G., Yanagawa, Y., Obata, K., Okano, H., Toida, K., Puche, A., Shipley, M.T., 2010. Molecular identity of periglomerular and short axon cells. J. Neurosci. 30, 1185-1196.

Kosaka, T., Hataguchi, Y., Hama, K., Nagatsu, I., Wu, J.Y., 1985. Coexistence of immunoreactivities for glutamate decarboxylase and tyrosine hydroxylase in some neurons in the periglomerular region of the rat main olfactory bulb: Possible

coexistence of gamma-aminobutyric acid (GABA) and dopamine. Brain Res. 343, 166–71.

Kosaka, T., Kosaka, K., 2007. Heterogeneity of nitric oxide synthase-containing neurons in the mouse main olfactory bulb. Neurosci. Res. 57, 165-178.

Kosaka, T., Kosaka, K., 2008a. Heterogeneity of parvalbumin-containing neurons in the mouse main olfactory bulb, with special reference to short-axon cells and βIV-spectrin positive dendritic segments. Neurosci. Res. 60, 56-72.

Kosaka, T., Kosaka, K., 2008b. Tyrosine hydroxylase-positive GABAergic juxtaglomerular neurons are the main source of the interglomerular connections in the mouse main olfactory bulb. Neurosci. Res. 60, 349-354.

Kosaka, T., Kosaka, K., 2009. Two types of tyrosine hydroxylase positive GABAergic juxtaglomerular neurons in the mouse main olfactory bulb are different in their time of origin. Neurosci. Res. 64, 436-441.

Kosaka, T., Kosaka, K., 2010. Heterogeneity of calbindin-containing neurons in the mouse main olfactory bulb: I. General description. Neurosci. Res. 67, 275–292.

Kosaka, T., Kosaka, K., 2011. “Interneurons” in the olfactory bulb revisited. Neurosci. Res. 69, 93-99.

Kosaka, K., Kosaka, T., 2013. Secretagogin-containing neurons in the mouse main olfactory bulb. Neurosci. Res. 77, 16-32.

Kosaka, K., Kosaka, T., 2016. Neuronal organization of the main olfactory bulb

revisited. Anat. Sci. Int. 91, 115-127. doi: 10.1007/s12565-015-0309-7.

Kosaka, T., Kosaka, K., Hataguchi, Y., Nagatsu, I., Wu, J.Y., Ottersen, O.P., Storm-Mathisen, J., Hama, K., 1987. Catecholaminergic neurons containing GABA-like and/or glutamic acid decarboxylase-like immunoreactivities in various brain regions of the rat. Exp. Brain Res. 66, 191-210.

Liberia, T., Blasco-Ibáñez, J.M., Nácher, J., Varea, E., Zwafink, V., Crespo, C., 2012. Characterization of a population of tyrosine hydroxylase-containing interneurons in the external plexiform layer of the rat olfactory bulb. Neuroscience 217, 140-153.

Liu, S., Puche, A. C., Shipley, M. T., 2016. The interglomerular circuit potently inhibits olfactory bulb output neurons by both direct and indirect pathways. J. Neurosci. 36, 9604-9614.

Maher, B.J., Westbrook, G.L., 2008. Co-transmission of dopamine and GABA in periglomerular cells. J. Neurophysiol. 99, 1559-1564.

Matsushita, N., Okada, H., Yasoshima, Y., Takahashi, K., Kiuchi, K., Kobayashi, K., 2002. Dynamics of tyrosine hydroxylase promotor activity during midbrain dopaminergic neuron development. J. Neurochem. 82, 295-304.

Nagatsu, I. 1983. Immunohistochemistry of biogenic amines and immunoenzyme-histocytochemistry of catecholamine-synthesizing enzymes. In: Parvez, S.,

Nagatsu, T., Nagatsu, I., Parvez, H., (Eds.), Methods in biogenic amine research. Elsevier Science, Amsterdam, pp. 873-909.

Nagayama, S., Homma, R., Imamura, F., 2014. Neuronal organization of olfactory bulb circuits. Front. Neural Circuits 08-00098:1-19.

Panzanelli, P., Fritsch, J.M., Yanagawa, Y., Obata, K., Sassoè-Pognetto, M., 2007. GABAergic phenotype of periglomerular cells in the rodent olfactory bulb. J. Comp. Neurol. 502, 990–1002.

Parrish-Aungst, S., Kiyokage, E., Szabo, G., Yanagawa, Y., Shipley, M.T., Puche, A.C., 2007. Quantitative analysis of neuronal diversity in the mouse olfactory bulb. J, Comp, Neurol, 501, 825–836.

Pignatelli, A., Ackman, J.G., Vigetti, D., Beltrami, A. P., Zucchini, S., Belluzzi, O., 2009. A potential reservoir of immature dopaminergic replacement neurons in the adult mammalian olfactory bulb. Pflugers Arch.-Eur. J. Physiol. 457, 899-915.

Pignatelli, A., Belluzzi, O., 2017. Dopaminergic neurons in the main olfactory bulb: an overview from an electrophysiological perspective. Front. Neuroanat. 11, 7. doi: 10.3389/fnana.2017.00007

Pignatelli, A., Kobayashi, K., Okano, H., Belluzzi, O., 2005. Functional properties of dopaminergic neurons in the mouse olfactory bulb. J. Physiol. 564, 501-514.

Pinching, A. J., Powell, T. P. S., 1971. The neuron types of the glomerular layer of the

olfactory bulb. J. Cell Sci. 9, 305–345.

Ramón y Cajal, S., 1995. Histology of the nervous system of man and vertebrates. (Translated by N. Swanson and L. W. Swanson from the French; French edition, Histologie du Système Nerveux de l'homme et des Vertébrés, reviewed and updated by the author, translated from the Spanish by Dr. L. Azoulay, published in 1911) New York, Oxford. Oxford University Press.

Sawamoto, K., Nakao, N., Kobayashi, K., Matsushita, N., Takahashi, H., Kakishita K., Yamamoto, A., Yoshizaki, T., Terashima, T., Murakami, F., Itakura, T., Okano, H. 2001. Visualization, direct isolation, and transplantation of midbrain dopaminergic neurons. Proc. Natl. Acad. Sci. USA. 98, 9423-6428.

Shao, Z., Liu, S., Zhou, F., Puche, A.C., Shipley, M.T., 2019. Receiprocal inhibitory glomerular circuits contribute to excitation-inhibition balance in the mouse olfactory bulb. eNeuro. https://doi.org/10.1523/ENEURO.0048-19.2019.

Vaaga, C.E., Yorgason, J.T., Williams, J.T., Westbrook, G.L., 2017. Presynaptic gain control by endogenous cotransmission of dopamine and GABA in the olfactory bulb. J. Neurophysiol. 117, 1163-1170.

Figure legends

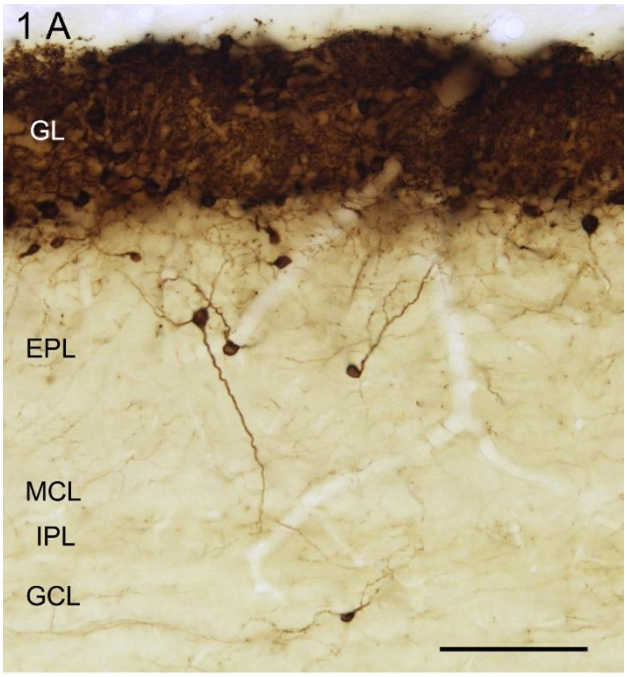

Figure 1 A, B: photomicrograph of a TH immunostained 50 μm thick horizontal section (**A**) and a composite of camera lucida drawings of a tangential section passing through the border between the GL and EPL of the control MOB (**B**). In **B** two small periglomerular cells (1, 2) and one large periglomerular cell (3) are shown. A dashed line indicates the contour of a glomerulus. A red-colored process of cell 3 is axon. Scale

bar in A: 100 μm. Scale bar in B: 10 μm.

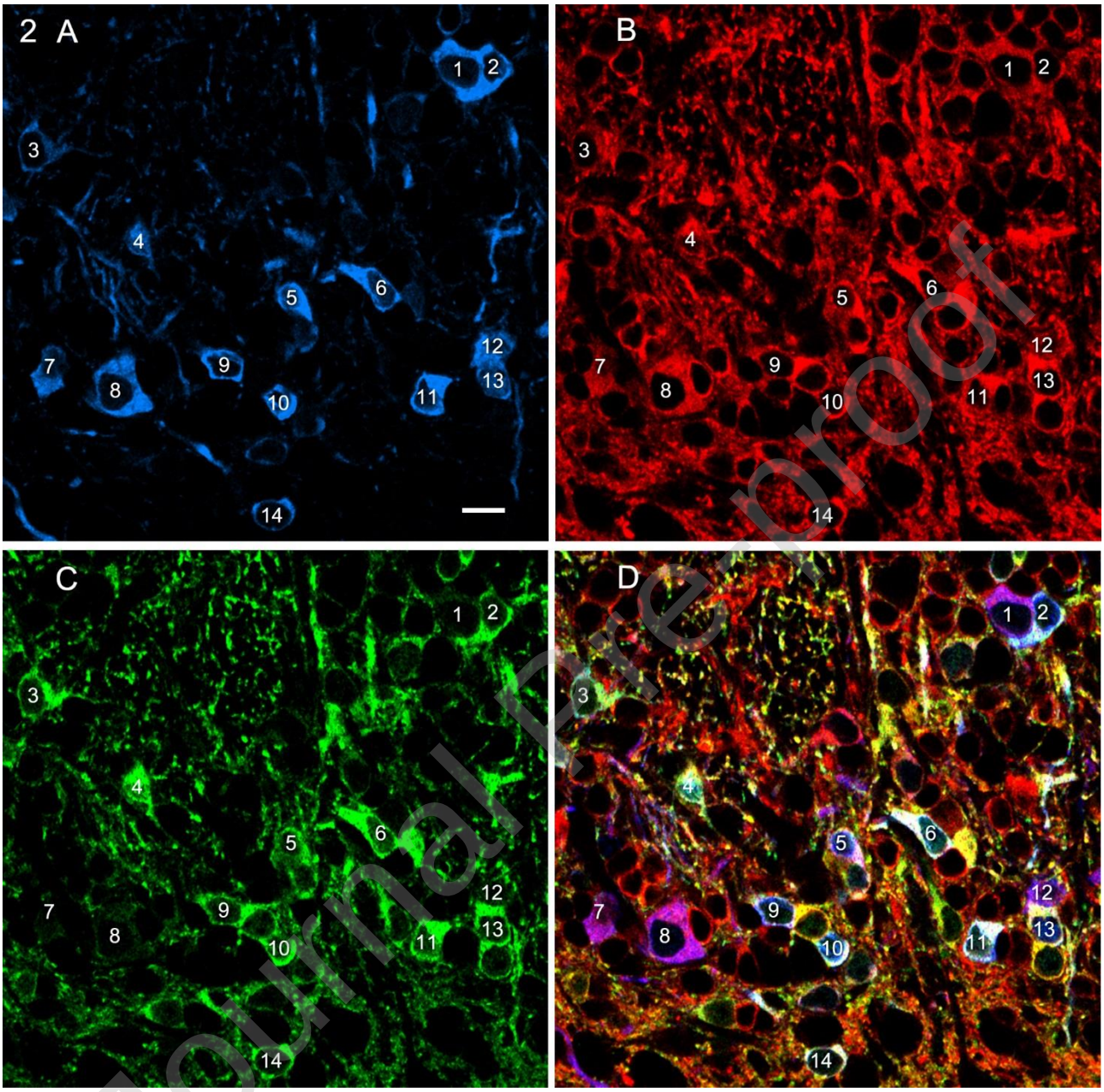

Figure 2 A-D; Pseudo-colored CLSM partial projection images of a horizontal section triple-immunostained for TH (**A**, blue in **D**), GAD67 (**B**, red in **D**) and GAD65 (**C**, green in **D**). TH positive cells 1, 7 and 8 are GAD 67 positive but nearly GAD65 negative. TH positive cells 2-6, 9-11, 13 and14 are both GAD67 and GAD65 positive. TH positive cell

12 is faintly GAD67 positive and GAD65 negative. Scale bar in **A** is 10 μm, which is also applicable to **B**-**D**.

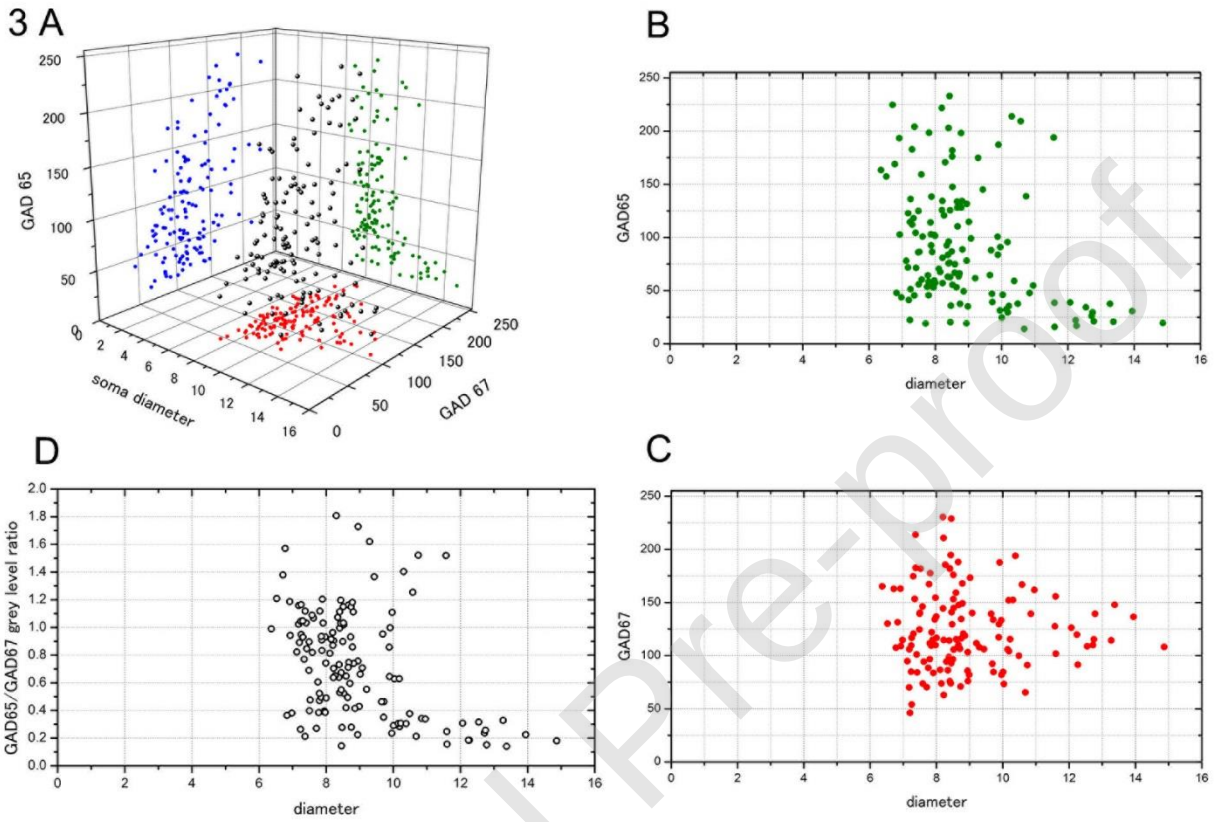

Figure 3 A-D; Scattergrams of the relationships of the immunointensities (GAD 65, **B** and green in **A**: GAD 67, **C** and red in **A**) and soma diameters of individual TH positive juxtaglomerular neurons. **D** shows the relationship between the GAD65/GAD67 intensity ratio and the soma diameter of individual TH positive juxtaglomerular neurons. Totally 134 TH positive juxtaglomerular neurons obtained from the CLSM images were analyzed.

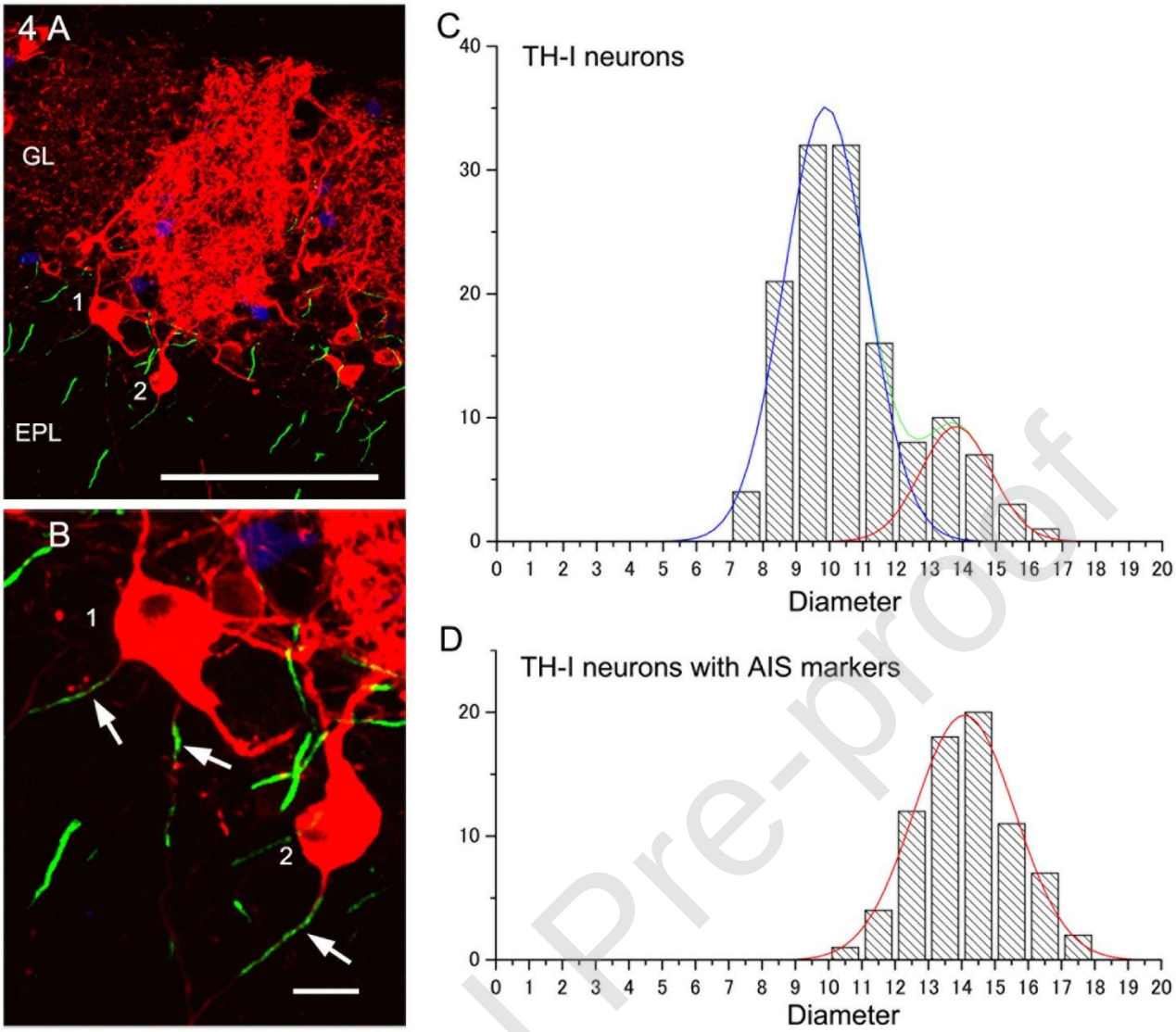

Figure 4 A, B; pseudo-colored CLSM partial projection images of the GL triple-immunostained for AnkG (green), TH (red) and SCGN (blue). Cells 1 and 2 are large periglomerular cells with axons with AnkG positive AISs (arrows). Cell 1 has two axons and cell 2 has one. Scale bar in A: 100 μm. Scale bar in B: 10 μm.

C, D: Histograms of the soma diameter distributions of the TH positive juxtaglomerular neurons (**C**) and the TH positive juxtaglomerular neurons with AnkG positive AISs (**D**). Histograms are obtained from the same sets of image stacks

of one 8w old mouse triple-immunostained for TH, AnkG and SCGN. Ordinate, number of somata. Abscissa, area equivalent diameters of somata (μm). Gaussian curves (colors) were created with the curve fitting procedure using Origin 7J. In **C** the histogram of size distribution (green) is fitted with two Gaussian curves (blue and red). In **D** histogram is fitted with one Gaussian curve (red).

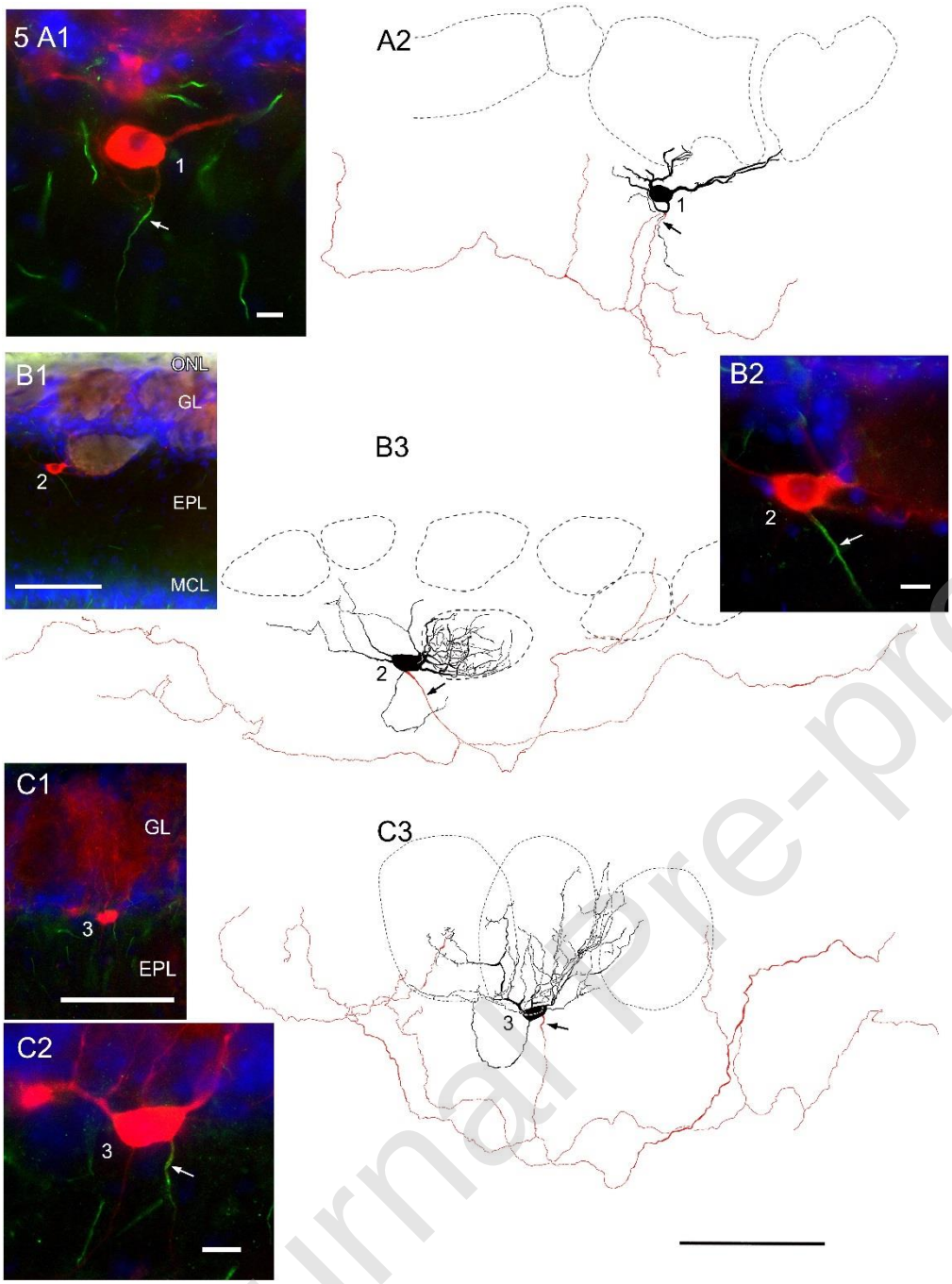

Figure 5: pseudo-colored photographs **(A1, B1, B2, C1, C2)** and camera lucida drawings **(A2, B3, C3)** of large periglomerular cells (LPG cells) in the control MOBs **(A1, 2)** and deprived MOBs **(B1-3, C1-3)**. **A1**: pseudo-colored photomontage of LPG cell 1 at the GL-EPL border triple-stained for AnkG (green), TH (red) and DAPI (blue). **A2**: camera lucida drawing of cell 1, which was processed for ABC-DAB method for TH.

AnkG positive AIS of cell 1 is indicated by arrow, which arises from a dendritic process. Axon (red) is also indicated in **A2** by arrow. Dashed lines outline individual glomeruli. **B1:** photomontage of cell 2 quadruple-stained for TH (red), AnkG (green), DAPI (blue) and OMP (grey). **B2**: higher magnification image of part of **B1** showing only 3 channels, TH (red), AnkG (green) and DAPI (blue). Arrow indicates AnkG positive AIS, which arises from the soma. **B3**: camera lucida drawing of cell 2, which was processed for ABC-DAB method for TH. Axon (red) is also indicated in **B3** by arrow. **C1**: photomontage of cell 3 triple-stained for TH (red), AnkG (green) and DAPI (blue). **C2**: higher magnification image of part of **C1**. Arrow indicates AnkG positive AIS. **C3**: camera lucida drawing of cell 3, which was processed for ABC-DAB method for TH. Axon (red) is also indicated in **C3** by arrow. Scale bars in **A1**, **B2** and **C2** are 10 μm. Scale bars in **B1** and **C1** are 100 μm. Scale bar at the bottom of this plate is 100 μm, which is applicable to **A2**, **B3** and **C3**.

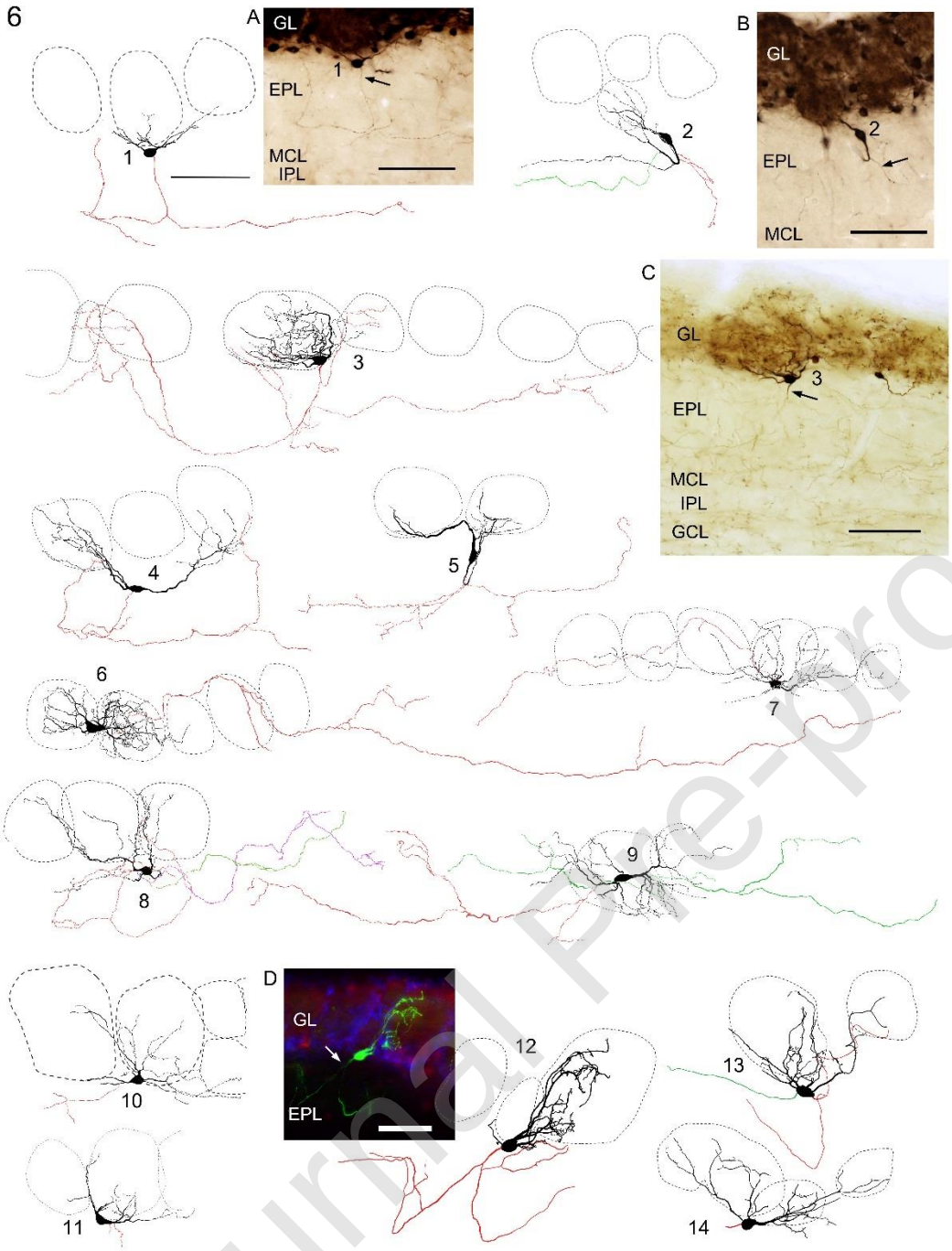

Figure 6 Cells 1, 2: camera lucida drawings of LPG cells in control MOBs immunostained for TH. **Insets A** and **B** are photomontages of **cells 1** and **2**, respectively. Arrows in insets indicate axons. **Cells 3-9:** camera lucida drawings of LPG cells in deprived MOBs. **Inset C** is photomontage of **cell 3**. Arrow in inset **C** indicates axon. **Cells 10, 11**: camera lucida drawings of BDA-labeled LPG cell in control MOB. **Cells 12-14:**

Neurolucida drawings of LY-labeled LPG cells in fixed slices of TH-GFP MOBs. **Inset D:** pseudo-colored photomontage of **cell 12** stained for LY (green), TH (red) and DAPI (blue). Arrow indicates axon. In camera lucida and Neurolucida drawings axons are shown in color, red, green and purple. **Cells 2**, **9** and **13** have 2 axons (red, green) and **cell 8** has 3 axons (red, green and purple). Dashed lines outline individual glomeruli. Scale bar at **cell 1** is 100 μm, which is applicable to all drawings. Scale bars in insets **A-D** are 100 μm.

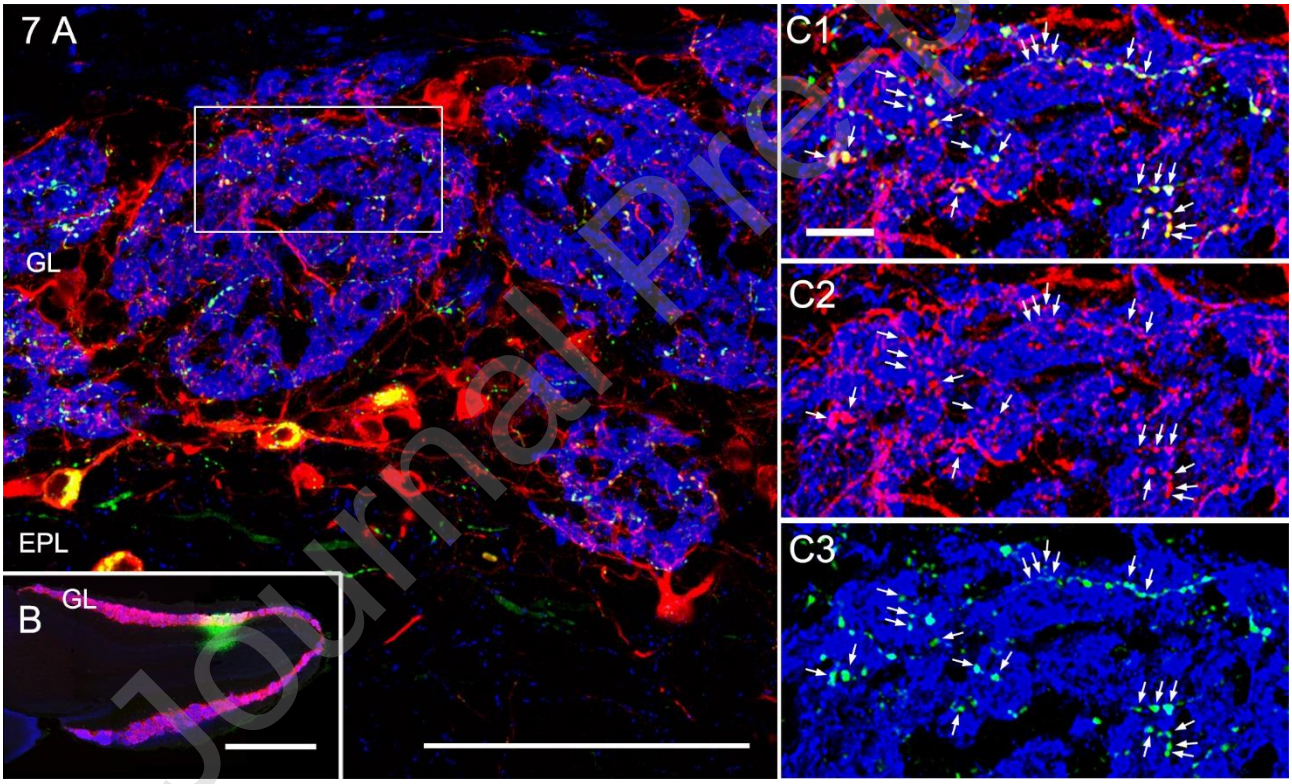

Figure 7. A, B, C: Pseudo-colored CLSM partial projection images of triple-immunostained section for TH (red), cholera toxin B subunit (CTB; green) and vesicular glutamate transporter 2 (VGluT2; blue), a marker for olfactory nerves and

terminals. Mouse MOB. Area shown in **A** is about 500μm rostral from the injected site (**B**). The area outlined by a rectangle in **A** is shown in **C1-3** at a higher magnification displaying merged three channels (**C1**) and two different channels (**C2**, **3**). In **C2** TH (red) and VGluT2 (blue) channels, and in **C3** CTB (green) and VGluT2 (blue) channels are shown, respectively. Small arrows in **C1-3** indicate intraglomerular CTB-labeled TH positive puncta. CTB-labeled TH positive puncta are mainly located in the VGluT2 positive ON zone. Scale bars are 100 μm in **A**, 1 mm in **B**, 10 μm in **C1** (applicable to **C2** and **C3**).

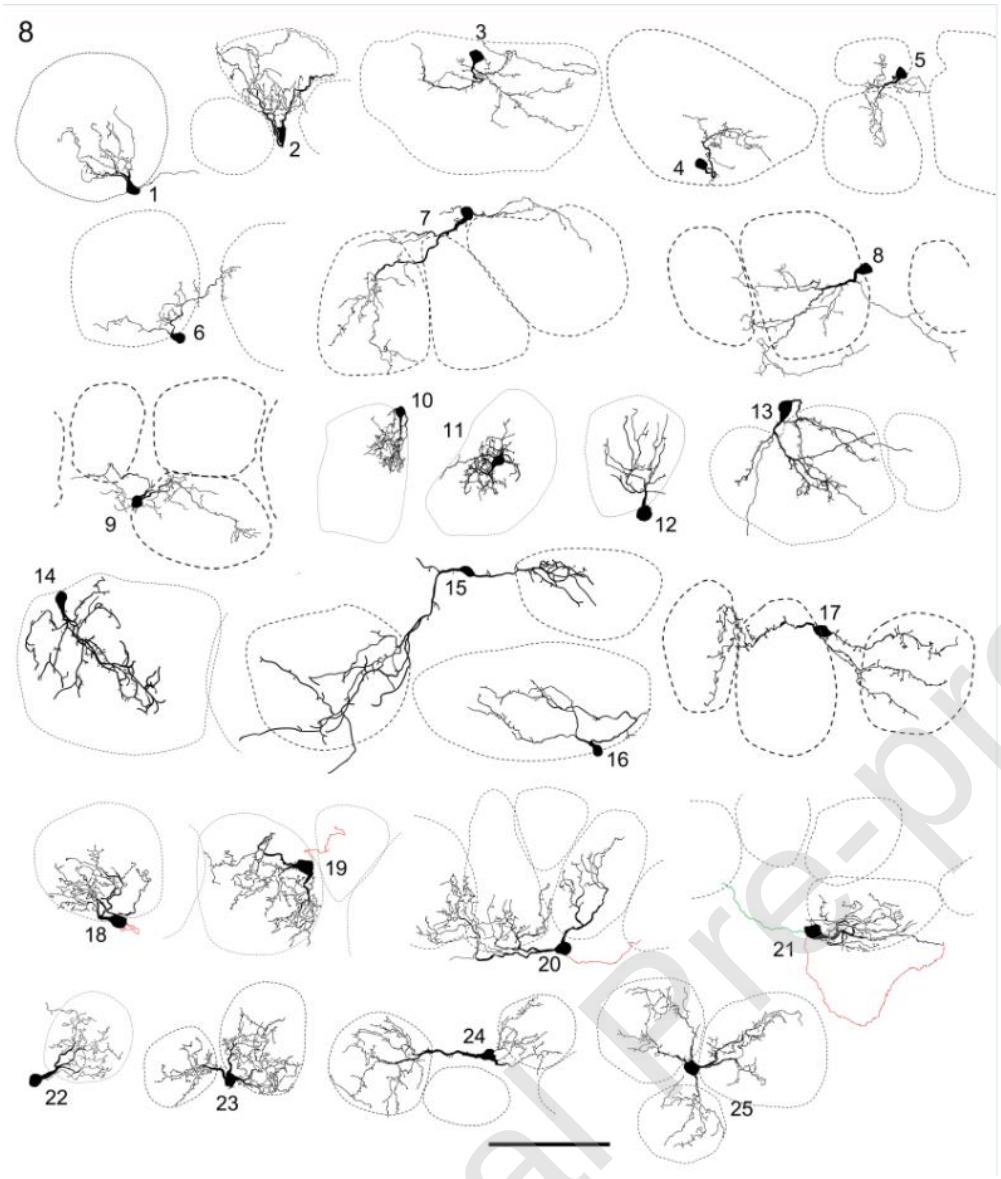

Figure 8 Cells 1-9: camera lucida drawings of BDA-labeled small periglomerular cells (SPG cells) in control MOBs. **Cells 10-13**: Neurolucida drawings of LY-labeled SPG cells in fixed slices of TH-GFP MOBs. **Cells 14-16:** Neurolucida drawings of biocytin-labeled SPG cells in live slices of TH-GFP MOBs. **Cell 17**: camera lucida drawing of biocytin-labeled SPG cell in live slice of TH-GFP MOB. **Cells 18-25:** camera lucida drawings of SPG cells immunostained for TH in deprived MOBs. **Cells 18-21** have axons: **cells 18-20** have one axon (red), and **cell 21** has two axons (red and green).

Dashed lines outline individual glomeruli. Scale bar is 100 μm which is applicable to all drawings.

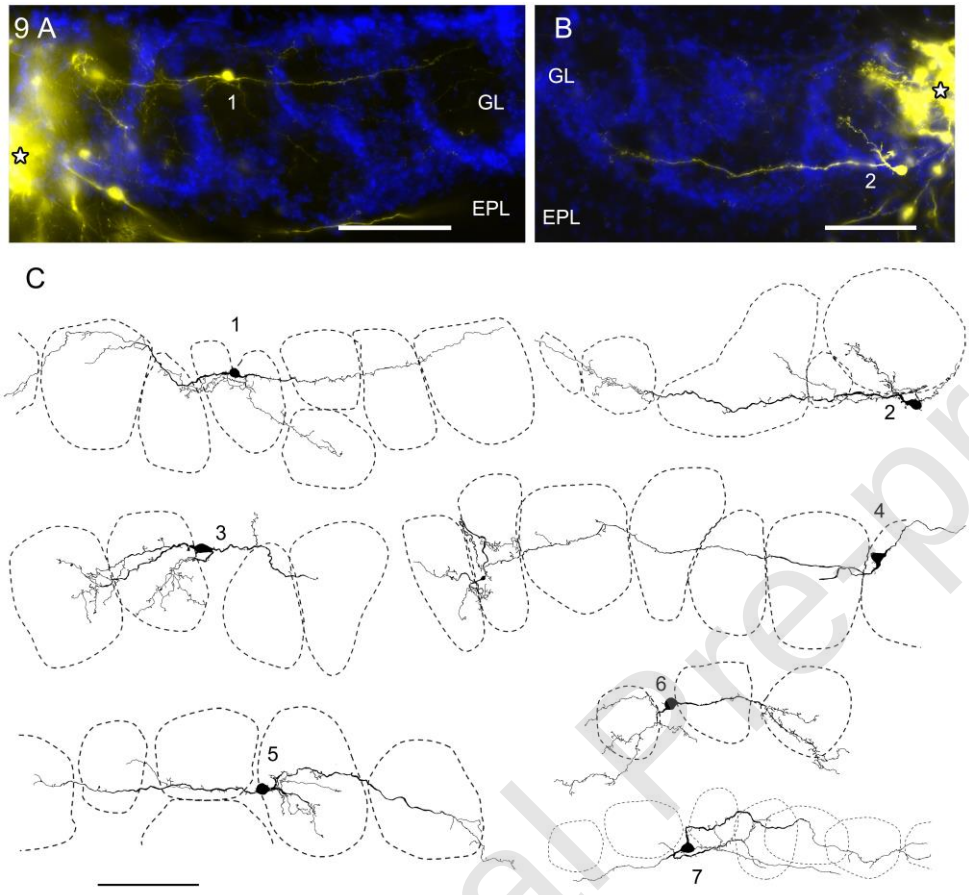

Figure 9 A, B: Pseudo-colored photomontages of BDA-labeled transglomerular cells corresponding to cells 1 and 2 shown in **C**, respectively. Horizontal sections of TH-GFP mice double-labeled with BDA (yellow) and DAPI (blue). Stars: injection sites. **C:** camera lucida drawings of transglomerular cells. **Cells 1-5**: BDA-labeled cells. **Cell 6**: biocytin-labeled transglomerular cell in live slice of TH-GFP MOB. **Cell 7**: TH immunostained transglomerular cell in deprived MOB. Dashed lines outline

individual glomeruli. Scale bars in **A, B** and **C** are 100 μm.

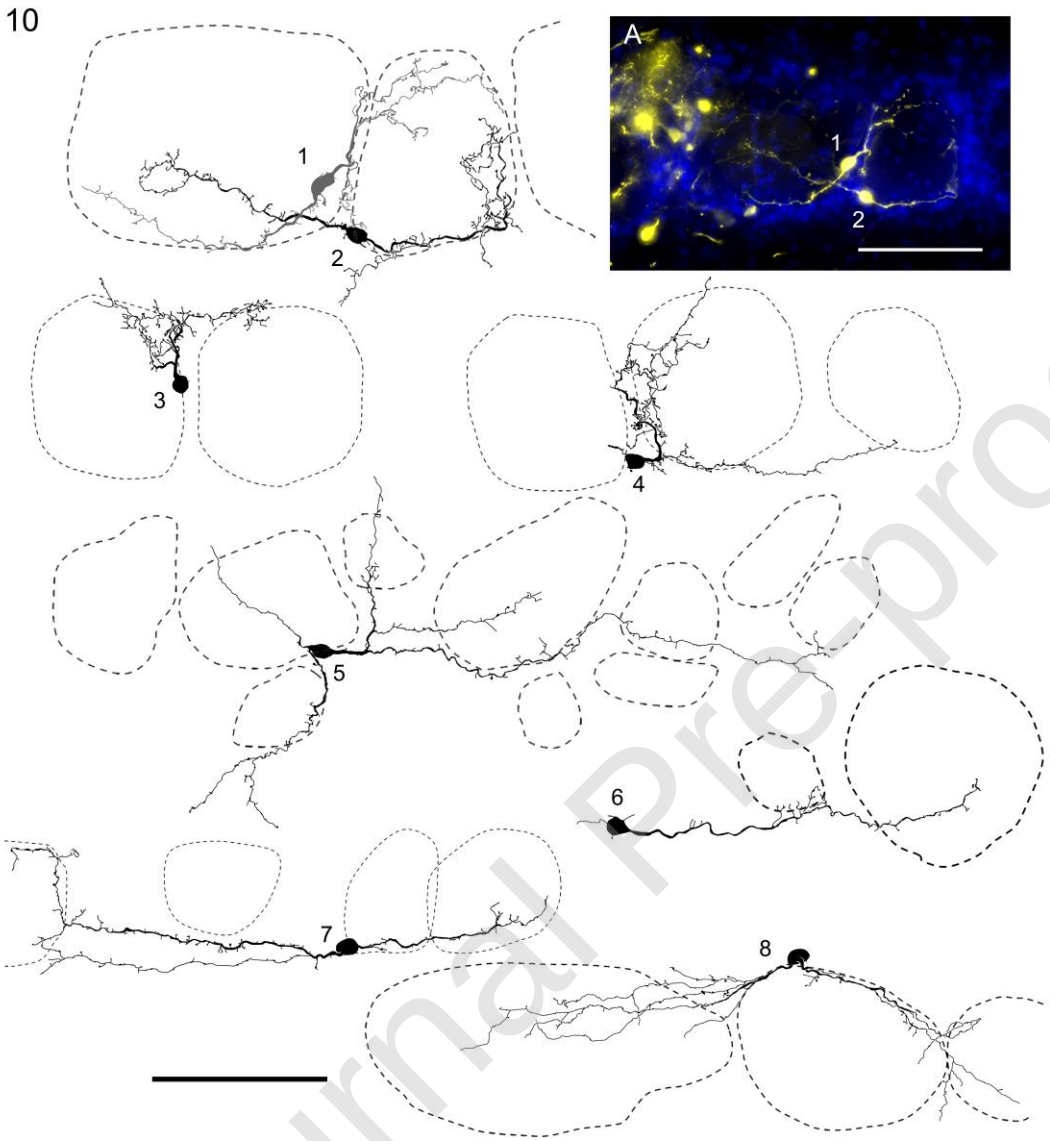

Figure 10 Camera lucida drawings of incrusting cells. **Cells 1-5**: BDA-labeled cells. **Cell 6**: biocytin-labeled incrusting cell in live slice of TH-GFP MOB. **Cells 7, 8**: TH immunostained incrusting cells in deprived MOBs. **Cell 8** shows rather prominent tuft-like branches near the center of a glomerulus, and thus somewhat atypical of the incrusting cell. Inset **A** is pseudo-colored photomontage of **cells 1** and **2** stained for

BDA (yellow) and DAPI (blue). Dashed lines outline individual glomeruli. Scale bar is 100 μm which is applicable to drawings of **Cells 1-8**. Scale bar in inset **A** is 100 μm.

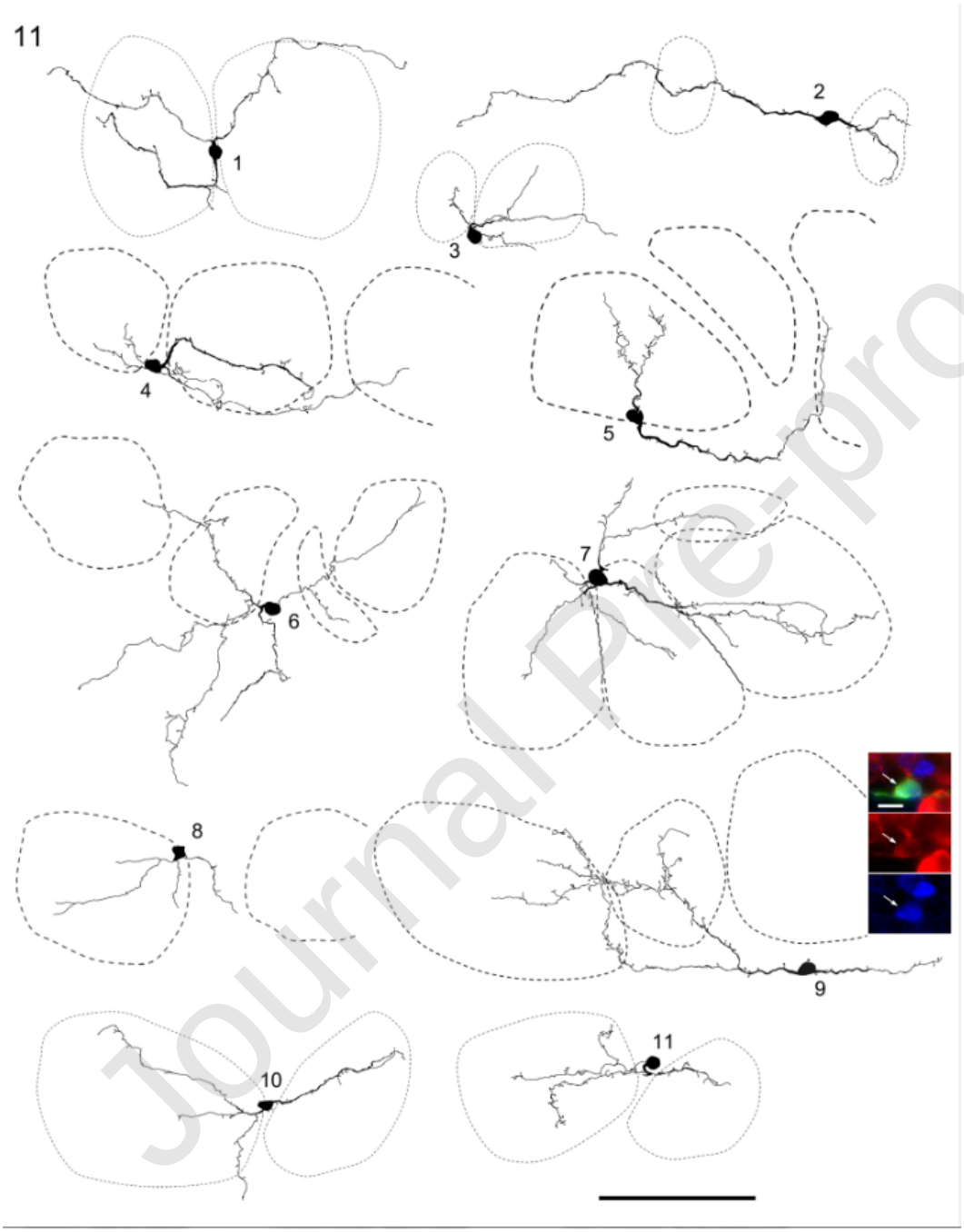

Figure 11 Camera lucida drawings of other unclassified cells in the GL. BDA-labeled cells.

Cells 9-11 were confirmed to be also SCGN positive. Inset: pseudo-colored

photographs of soma (arrow) of **cell 9** in merged and individual channels (BDA, green; TH, red; SCGN, blue). Dashed lines outline individual glomeruli. Scale bar is 100 μm. Scale bar in inset is 10 μm.

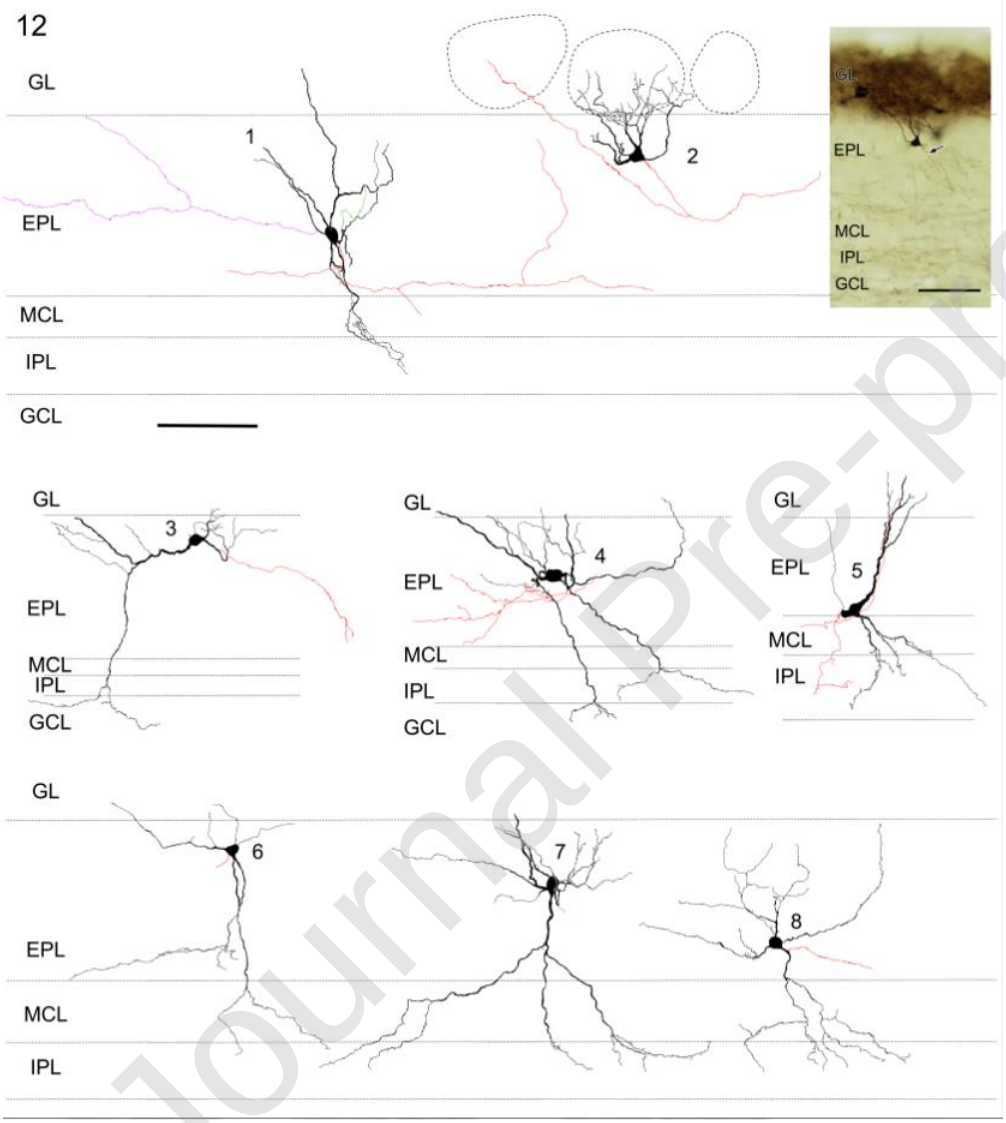

Figure 12 Camera lucida drawings of TH positive large cells with axons (red) in the EPL. **Cell 1** has three axons (red, green, purple). **Cells 1, 3-8** were observed in control MOBs. **Cell 2** is a displaced LPG cell in a deprived MOB. Inset is a photomicrograph of **cell**

2. Arrow in inset indicates axon. Dashed lines indicate borders of layers. Dashed lines shown in **cell 2** outline individual glomeruli. Scale bar is 100 μm which is applicable to all drawings. Scale bar in inset is 100 μm.

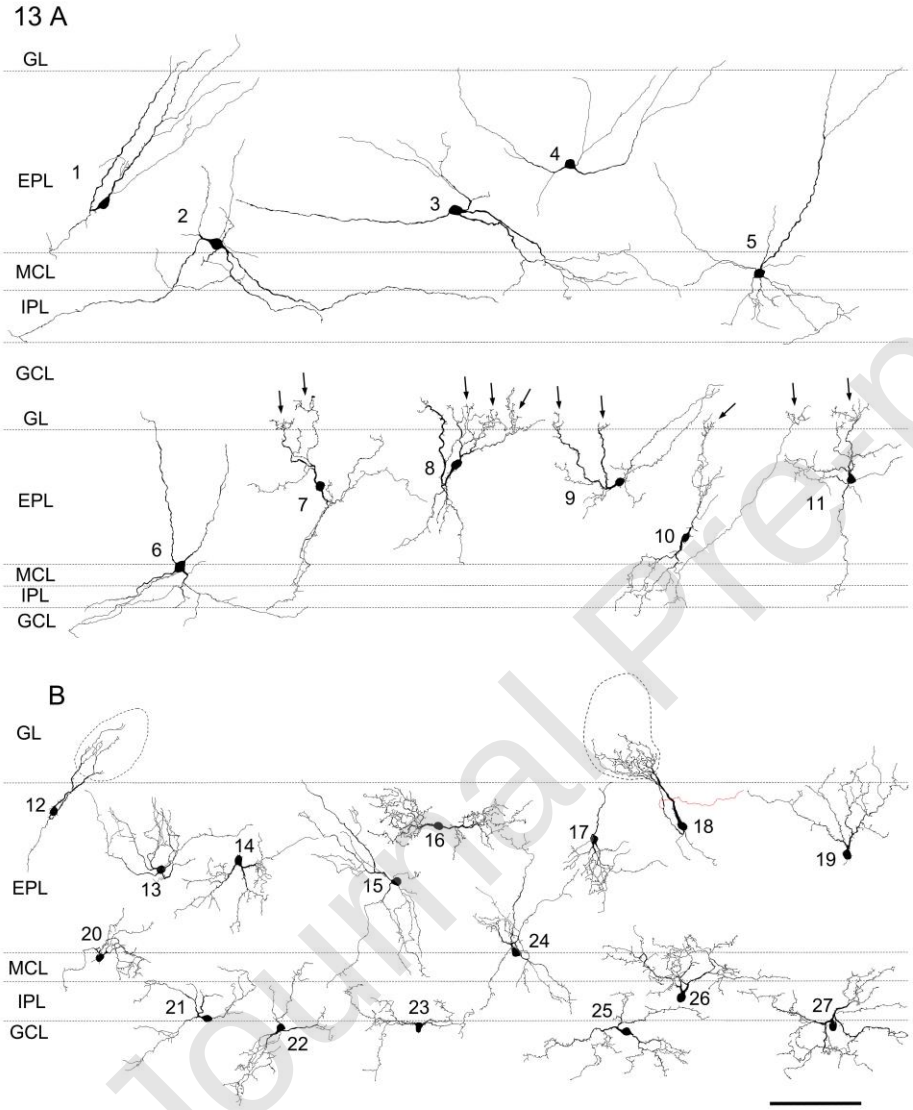

Figure 13 A: Camera lucida drawings of TH positive large cells in the EPL~MCL. **Cells 1-5** in control MOBs. **Cells 6-11** in deprived MOBs. **Cells 7-11** show small tuft-like dendritic branches (arrows) in the GL. Dashed lines indicate borders of layers. **B:** Camera

lucida drawings of TH positive relatively small cells in the EPL~GCL. **Cells 12-17** and **20-24** in control MOBs. **Cells 18, 19** and **25-27** in deprived MOBs. **Cells 12** and **18** are displaced SPG cells. **Cell 18** has an axon (red). Scale bar is 100 μm, which is applicable to all drawings.